Joint Transmit and Receive Filters Design for Multiple-Input Multiple-Output (MIMO) Systems

Keun Chul Hwang and Kwang Bok (Ed) Lee, *Member, IEEE*

***Abstract*—Multiple transmit (Tx) and multiple receive (Rx) antennas systems, referred to as multiple-input multiple-output (MIMO) systems, have been proposed to achieve higher data rates in wireless communication systems. In this paper, we investigate joint design of transmitter and receiver for the MIMO system when the channel information is available at both transmitter and receiver. We discuss the problem concerning the design of Tx and Rx filters with the aim of minimizing the bit-error probability (BEP). We derive the optimum Tx and Rx filters when the number of data symbols is two. For a general number of data symbols, we derive a Tx and Rx filters design criterion referred to as *equal signal-to-noise plus interference ratio (SNIR) criterion*, and propose Tx and Rx filters based on this equal SNIR criterion. The performance of the proposed filter is compared with that of the conventional minimum mean-squared error (MMSE) filter. Performance analysis shows that the proposed filter provides a significant improvement over the MMSE filter in BEP and spectral efficiency.**

***Index Terms*—Beamforming, diversity, multiple-input multiple-output (MIMO), performance, spatial filter.**

I. Introduction

MULTIPLE transmit (Tx) and multiple receive (Rx) antennas, referred to as multiple-input multiple-output (MIMO), are known for significantly improving the capacity of wireless communication systems [1]–[4]. Especially, it is well known that the achievable capacity of MIMO links increases almost linearly with the minimum number of transmit and receive antennas in rich scattering environments. Due to this potentially significant capacity improvement, MIMO systems may be applied in high data rate service for the next-generation wireless communication systems.

A MIMO system can be classified according to whether or not the channel state information (CSI) is available at either the transmitter or the receiver. Most existing MIMO systems assume that the CSI is available only at the receiver. However, MIMO systems can further enhance performance when CSI is available at both transmitter and receiver [5]. Obviously, the best performance can be obtained when CSI is perfectly known at both transmitter and receiver, which is difficult to achieve because of an error in channel estimation or the time-varying channel response. Consequently, performance improvement obtained in practice depends on the accuracy of CSI. Several methods for accurate CSI at the transmitter and receiver are found throughout the literature. The CSI at the transmitter can be obtained by using a feedback channel in frequency-division duplex (FDD) system, or can be estimated from the uplink channels in time-division duplex (TDD) system. At the receiver, CSI may be obtained by the well-known channel estimation techniques.

When CSI is known at both transmitter and receiver, this CSI can be used to design efficient transmit and receive filters. Several transmit and receive filters have been proposed to improve the performance of MIMO systems. In [6], the optimum Tx and Rx filters that minimize the mean-squared error were derived for a strictly band-limited system, and a more complete analysis based on a frequency-domain analysis appeared in [7] and [8]. In [9], the optimum Tx and Rx filters were derived using the minimum mean-squared error (MMSE) criterion, with which the sum of the mean-squared errors between the input data symbols and the estimated data symbols is minimized. In [10], the authors generalized their previous work [8], and proposed the Tx and Rx filters that minimize the weighted sum of mean-squared errors. All the works in [6]–[10] have been conducted based on the MMSE criterion. However, since the MMSE is not directly related to bit-error probability (BEP), the MMSE filter does not ensure the best BEP performance. Recently, in [11], a minimum BEP filter for a single-input single-output (SISO) system was investigated, and has shown to yield significant performance improvement over the MMSE filter.

In this paper, we investigate the design of Tx and Rx filters for the MIMO system with the purpose of minimizing the BEP instead of MMSE. We derive the optimum Tx and Rx filters when the number of data symbols is two. For a general number of data symbols, we derive a Tx and Rx filters design criterion, referred to as *equal signal-to-noise plus interference ratio (SNIR) criterion*, and propose Tx and Rx filters based on this equal SNIR criterion. The remainder of this paper is organized as follows. Section II describes a MIMO system model. In Section III, a Tx and Rx filters optimization problem is formulated, and the optimum Tx and Rx filters for two data symbols are derived. The equal SNIR criterion and the proposed Tx and Rx filters are described in Section IV, and the performance of the proposed filter is presented in Section V. The spectral efficiency of the proposed filter and practical issue are discussed in Section VI. Finally, some conclusions are drawn in Section VII.

Manuscript received April 18, 2003; revised January 19, 2004; accepted April 8, 2004. The editor coordinating the review of this paper and approving it for publication is R. Murch.

K. C. Hwang was with the Wireless Networking and Communications Group (WNCG), Department of Electrical and Computer Engineering, The University of Texas at Austin, Austin, TX 78712-0240 USA. He is now with Samsung Electronics Inc., Suwon, Kyunggi-do 442-600, Korea (e-mail: keunchul.hwang@samsung.com).

K. B. Lee is with the School of Electrical Engineering and Computer Science, Seoul National University, Seoul 151-742, Korea (e-mail: klee@snu.ac.kr).

Digital Object Identifier 10.1109/TWC.2005.846999

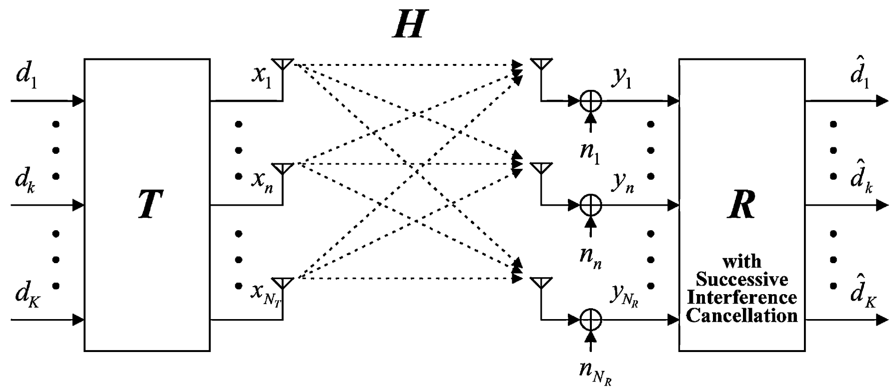

Fig. 1. System model.

II. Multiple-Input Multiple-Output (MIMO) System

A MIMO system with N_T transmit (Tx) antennas and N_R receive (Rx) antennas is considered. At the transmitter, multiple data symbols are constructed using the same modulation scheme, and passed through the Tx filter. These filtered data symbols are simultaneously transmitted through N_T transmit antennas, and received at N_R receive antennas. At the receiver, each received signal is corrupted by an additive white Gaussian noise (AWGN), and processed with the Rx filter. A baseband equivalent MIMO system model is shown in Fig. 1. The transmitted signal may be expressed in vector form

$$\boldsymbol{x} = \sqrt{P}\boldsymbol{T}\boldsymbol{d} \tag{1}$$

where $\boldsymbol{x} = [x_1 x_2 \ldots x_{N_T}]^T$ denotes the transmitted signal vector, and the superscript ^{T} denotes the transpose. $\boldsymbol{d} = [d_1 d_2 \ldots d_K]^T$ denotes the data symbol vector, where K denotes the number of data symbols, which is assumed to be $K = \min(N_T, N_R)$. Although the Tx and Rx filters can be applied to any modulation scheme, we assume, for analytical simplicity, that d_k's are the M-ary quadrature amplitude modulated (M-QAM) data symbols with $E[\boldsymbol{d}\boldsymbol{d}^H] = \boldsymbol{I}_K$, where $E[\cdot]$ is the expectation operation, the superscript ^{H} denotes the conjugate transpose, and $\boldsymbol{I}_n$ denotes the $n \times n$ identity matrix. In this paper, we consider an equal power transmission, and the transmit power is assumed to be the same as P for all data symbols. Note that the total Tx power is $K \cdot P$. A Tx filter $\boldsymbol{T}$ consists of K Tx weight vectors $\boldsymbol{t}_k$, and may be expressed as

$$T = [\boldsymbol{t}_1 \quad \boldsymbol{t}_2 \quad \cdots \quad \boldsymbol{t}_K] \tag{2}$$

where $\boldsymbol{t}_k = [t_{1,k} t_{2,k} \ldots t_{N_T,K}]^T$ denotes a Tx weight vector for the data symbol d_k. Note that as a consequence of applying the Tx weight vector $\boldsymbol{t}_k$, the transmit power may fluctuate. To maintain consistency in the transmit power for various N_T, we normalize the Tx weight vector such that

$$||\boldsymbol{t}_k||^2 \triangleq \sum_{i=1}^{N_T} |t_{i,k}|^2 = 1, \qquad \forall k. \tag{3}$$

We assume that the transmitted signal experiences frequency-flat Rayleigh fading for all $N_T \cdot N_R$ transmit–receive antenna pairs. Each channel response is assumed to vary slowly enough to be regarded as constant throughout the data symbol duration. In this case, the channel responses may be integrated in a matrix form

$$\boldsymbol{H} = \begin{bmatrix} h_{1,1} & \cdots & h_{1,N_T} \\ \vdots & \ddots & \vdots \\ h_{N_R,1} & \cdots & h_{N_R,N_T} \end{bmatrix} \tag{4}$$

where $h_{i,j}$ denotes the channel response from the jth Tx antenna to the ith Rx antenna. The channel responses $h_{i,j}$'s are assumed to be independent and identically distributed (i.i.d.) zero-mean circular complex Gaussian random variables with unit variance. The channel matrix $\boldsymbol{H}$ is assumed to be perfectly known at both transmitter and receiver. The received signal vector $\boldsymbol{y} = [y_1 \ y_2 \ \ldots \ y_{N_R}]^T$ may be expressed as

$$\boldsymbol{y} = \boldsymbol{H}\boldsymbol{x} + \boldsymbol{n} \tag{5}$$

where $\boldsymbol{n} = [n_1 \ n_2 \ \ldots \ n_{N_R}]^T$ is an AWGN vector, whose elements are i.i.d. zero-mean circular complex Gaussian random variables with variance of σ_0^2.

At the receiver, the received signals pass through the Rx filter $\boldsymbol{R}$, which consists of K Rx weight vectors: $\boldsymbol{R} = [\boldsymbol{r}_1 \ \boldsymbol{r}_2 \ \ldots \ \boldsymbol{r}_K]^H$, where $\boldsymbol{r}_k$ is an $N_R \times 1$ receive weight vector for the data symbol d_k. We assume that the decision order is in accordance with data index; d_1 is decided first, and then d_2 is decided next, and so on. A successive interference cancellation is employed to remove the interferences; when we decide d_k, the interference from the $k-1$ previously decided symbols is regenerated and canceled out. Generally, some of these $k-1$ previously decided symbols may be erroneous. These erroneous symbols may cause wrong cancellation, and in turn may cause successive decision errors to occur. This phenomenon is known as *error propagation*. For analytical simplicity, however, we assume that the $k-1$ decisions used in cancellation are error free. Thus, the decision variable for d_k may be expressed as

$$\hat{d}_k = \sqrt{P}\boldsymbol{r}_k^H \boldsymbol{H}\boldsymbol{t}_k d_k + \sum_{i=k+1}^{K} \sqrt{P}\boldsymbol{r}_k^H \boldsymbol{H}\boldsymbol{t}_i d_i + \boldsymbol{r}_k^H \boldsymbol{n} \tag{6}$$

where the first term denotes a desired signal, and the second and third terms are the interference from the undecided symbols and AWGN, respectively.

III. Minimum BEP Transmit and Receive Filters Opimization

In this section, we investigate the design of optimum Tx and Rx filters with the aim of minimizing the BEP. The Tx and Rx filters optimization is investigated in Subsection III-A, and the optimum Tx and Rx filters for the case of $K = 2$ are derived in Subsection III-B.

A. Transmit and Receive Filters Optimization

Based on the central limit theorem [12], the interference $\sum_{i=k+1}^{K} \sqrt{P} \boldsymbol{r}_k^H \boldsymbol{H} \boldsymbol{t}_i d_i$ in (6) can be approximated as a Gaussian distributed random variable for large K. Using this Gaussian approximation, the BEP may be written as [12]

$$\begin{aligned} \text{BEP} &= \frac{1}{K}\sum_{k=1}^{K} \text{BEP}_k \\ &\cong \frac{1}{K}\sum_{k=1}^{K}\left\{\frac{4\cdot(1-1/\sqrt{M})}{\log_2 M} Q\left(\sqrt{\frac{3}{M-1}\text{SNIR}_k}\right)\right\} \end{aligned} \tag{7}$$

where $Q(x)$ is a Gaussian tail integral defined as

$$Q(x) = (1/\pi)\int_0^{\pi/2} \exp(-x^2/(2\sin^2\theta))d\theta$$

[13], and BEP_k and SNIR_k, respectively, denote the BEP and the SNIR for the kth data symbol d_k. From (6), SNIR_k may be calculated as

$$\text{SNIR}_k = \frac{\boldsymbol{r}_k^H (\boldsymbol{H}\boldsymbol{t}_k)(\boldsymbol{H}\boldsymbol{t}_k)^H \boldsymbol{r}_k}{\boldsymbol{r}_k^H \boldsymbol{\Phi}_k \boldsymbol{r}_k} \tag{8}$$

where $\boldsymbol{\Phi}_k$ denotes the noise-plus-interference power defined as

$$\begin{aligned} \boldsymbol{\Phi}_k &\triangleq \frac{1}{P}E[\boldsymbol{n}\boldsymbol{n}^H] + \sum_{i=k+1}^{K} E\left[d_i d_i^H\right](\boldsymbol{H}\boldsymbol{t}_i)(\boldsymbol{H}\boldsymbol{t}_i)^H \\ &= \frac{1}{\Gamma}\boldsymbol{I}_{N_R} + \sum_{i=k+1}^{K}(\boldsymbol{H}\boldsymbol{t}_i)(\boldsymbol{H}\boldsymbol{t}_i)^H \end{aligned} \tag{9}$$

and $\Gamma \triangleq P/\sigma_0^2$ denotes the transmit signal-to-noise ratio (TxSNR).

It can be seen from (8) that the kth receive weight vector $\boldsymbol{r}_k$ affects only the kth SNIR SNIR_k. Thus, to minimize the BEP in (7), the receive weight vector $\boldsymbol{r}_k$ should maximize SNIR_k. According to the generalized eigenvalue problem [14], the receive weight vector $\boldsymbol{r}_k$ that maximizes SNIR_k in (8) may be expressed as

$$\boldsymbol{r}_k = \mu_k \boldsymbol{\Phi}_k^{-1}\boldsymbol{H}\boldsymbol{t}_k \tag{10}$$

where μ_k is an arbitrary constant that does not affect the SNIR_k. For simplicity, we set $\mu_k = 1$ for all k. Substituting (10) into (8), the SNIR_k may be expressed as

$$\begin{aligned} \text{SNIR}_k &= \boldsymbol{t}_k^H \boldsymbol{H}^H \boldsymbol{\Phi}_k^{-1} \boldsymbol{H}\boldsymbol{t}_k \\ &= \Gamma\cdot\left(\boldsymbol{t}_k^H\boldsymbol{H}^H\boldsymbol{H}\boldsymbol{t}_k\right) - \sum_{i=k+1}^{K}\frac{\left|\boldsymbol{t}_k^H\boldsymbol{H}^H\boldsymbol{\Phi}_i^{-1}\boldsymbol{H}\boldsymbol{t}_i\right|^2}{1+\left(\boldsymbol{t}_i^H\boldsymbol{H}^H\boldsymbol{\Phi}_i^{-1}\boldsymbol{H}\boldsymbol{t}_i\right)} \end{aligned} \tag{11}$$

where the second equality is derived using the relation (see Appendix A)

$$\boldsymbol{\Phi}_k^{-1} = \Gamma\boldsymbol{I}_{N_R} - \sum_{i=k+1}^{K}\frac{\boldsymbol{\Phi}_i^{-1}\boldsymbol{H}\boldsymbol{t}_i\boldsymbol{t}_i^H\boldsymbol{H}^H\boldsymbol{\Phi}_i^{-1}}{1+\left(\boldsymbol{t}_i^H\boldsymbol{H}^H\boldsymbol{\Phi}_i^{-1}\boldsymbol{H}\boldsymbol{t}_i\right)}. \tag{12}$$

Note that SNIR_k in (11) is expressed in terms of the Tx weight vectors rather than both Tx and Rx weight vectors. Accordingly, BEP in (7) may be considered as a function of the Tx weight vectors. Consequently, the Tx filter optimization may be accomplished by finding the Tx weight vectors that minimize the BEP cost function

$$J(\boldsymbol{t}_1, \boldsymbol{t}_2, \ldots, \boldsymbol{t}_K) = \sum_{k=1}^{K}\left\{Q\left(\sqrt{\frac{3}{M-1}\text{SNIR}_k}\right)\right\} \tag{13}$$

where the multiplying factor $4\cdot(1-1/\sqrt{M})/(K\cdot\log_2 M)$ in (7) is dropped since it is independent of the Tx weight vectors. After finding the optimum $\boldsymbol{t}_k$'s that minimize (13), the corresponding optimum $\boldsymbol{r}_k$'s may be obtained from (10). Although it is hard to derive a general solution for optimum $\boldsymbol{t}_k$'s, we can derive the optimum $\boldsymbol{t}_k$'s when the number of data symbols is two ($K = 2$), as shown in the next subsection.

Before going to the next subsection, let us define the eigenvalue decomposition of $\boldsymbol{H}^H\boldsymbol{H}$ [15]

$$\begin{aligned} \boldsymbol{H}^H\boldsymbol{H} &= [\boldsymbol{V} \quad \tilde{\boldsymbol{V}}]\begin{bmatrix}\boldsymbol{\Lambda} & \boldsymbol{0}\\ \boldsymbol{0} & \boldsymbol{0}\end{bmatrix}\begin{bmatrix}\boldsymbol{V}^H\\ \tilde{\boldsymbol{V}}^H\end{bmatrix} \\ &= \boldsymbol{V}\boldsymbol{\Lambda}\boldsymbol{V}^H \end{aligned} \tag{14}$$

where $\boldsymbol{V} = [\boldsymbol{v}_1 \ \boldsymbol{v}_2 \ \ldots \ \boldsymbol{v}_K]$ is an $N_T \times K$ unitary matrix, $\boldsymbol{v}_k$'s are eigenvectors that form the bases for the range space of $\boldsymbol{H}^H\boldsymbol{H}$, and $\tilde{\boldsymbol{V}} = [\tilde{\boldsymbol{v}}_1 \ \tilde{\boldsymbol{v}}_2 \ \ldots \ \tilde{\boldsymbol{v}}_{N_T-K}]$ is an $N_T \times (N_T - K)$ unitary matrix whose column vectors, $\tilde{\boldsymbol{v}}_k$'s, form the bases for the null space of $\boldsymbol{H}^H\boldsymbol{H}$. The matrix $\boldsymbol{\Lambda} = \text{diag}\{\lambda_1, \lambda_2, \ldots, \lambda_K\}$ is a $K \times K$ diagonal matrix, and λ_k denotes the kth largest eigenvalue of $\boldsymbol{H}^H\boldsymbol{H}$: $\lambda_1 \geq \lambda_2 \geq \cdots \geq \lambda_K$. Note that $\boldsymbol{v}_k$ is an eigenvector corresponding to the eigenvalue λ_k.

B. Optimum Transmit and Receive Filters When the Number of Data Symbols Is Two ($K = 2$)

When $K = 2$, two Tx weight vectors, $\boldsymbol{t}_1$ and $\boldsymbol{t}_2$, need to be optimized, and the cost function in (13) is given as

$$J(\boldsymbol{t}_1, \boldsymbol{t}_2) = Q\left(\sqrt{\frac{3}{M-1}\text{SNIR}_1}\right) + Q\left(\sqrt{\frac{3}{M-1}\text{SNIR}_2}\right) \tag{15}$$

where SNIR_1 and SNIR_2 may be expressed from (11) as

$$\text{SNIR}_1 = \Gamma\cdot\left(\boldsymbol{t}_1^H\boldsymbol{H}^H\boldsymbol{H}\boldsymbol{t}_1\right) - \frac{\Gamma^2\cdot\left(\boldsymbol{t}_1^H\boldsymbol{H}^H\boldsymbol{H}\boldsymbol{t}_2\boldsymbol{t}_2^H\boldsymbol{H}^H\boldsymbol{H}\boldsymbol{t}_1\right)}{1+\Gamma\cdot\left(\boldsymbol{t}_2^H\boldsymbol{H}^H\boldsymbol{H}\boldsymbol{t}_2\right)} \tag{16}$$

$$\text{SNIR}_2 = \Gamma\cdot\left(\boldsymbol{t}_2^H\boldsymbol{H}^H\boldsymbol{H}\boldsymbol{t}_2\right). \tag{17}$$

Note that SNIR_1 is a function of both $\boldsymbol{t}_1$ and $\boldsymbol{t}_2$, whereas SNIR_2 is a function of only $\boldsymbol{t}_2$. Hence, for a given $\boldsymbol{t}_2$, SNIR_2 may be considered as a fixed value, whereas SNIR_1 is a function of $\boldsymbol{t}_1$. Consequently, for a given $\boldsymbol{t}_2$, the Tx weight vector $\boldsymbol{t}_1$ should maximize the SNIR_1 so as that the cost function $J(\boldsymbol{t}_1, \boldsymbol{t}_2)$ can be minimized. According to the eigenvalue problem [14], for a given $\boldsymbol{t}_2$, the Tx weight vector $\boldsymbol{t}_1$ that maximizes SNIR_1 may be expressed as

$$\boldsymbol{t}_1 = \boldsymbol{ev}_{\max}[\boldsymbol{A}(\boldsymbol{t}_2)] \tag{18}$$

where $\boldsymbol{ev}_{\max}[\boldsymbol{X}]$ denotes the eigenvector associated with the maximum eigenvalue of $\boldsymbol{X}$, and the matrix $\boldsymbol{A}(\boldsymbol{x})$ is defined as

$$\boldsymbol{A}(\boldsymbol{x}) \triangleq \boldsymbol{H}^H\boldsymbol{H} - \frac{\Gamma \cdot (\boldsymbol{H}^H\boldsymbol{H}\boldsymbol{x}\boldsymbol{x}^H\boldsymbol{H}^H\boldsymbol{H})}{1+\Gamma\cdot(\boldsymbol{x}^H\boldsymbol{H}^H\boldsymbol{H}\boldsymbol{x})}. \tag{19}$$

Substituting $\boldsymbol{t}_1 = \boldsymbol{ev}_{\max}[\boldsymbol{A}(\boldsymbol{t}_2)]$ in (16), the SNIR_1 becomes a function of $\boldsymbol{t}_2$, and may be expressed as

$$\mathrm{SNIR}_1(\boldsymbol{t}_2) = \Gamma \cdot \lambda_{\max}[\boldsymbol{A}(\boldsymbol{t}_2)]$$

where $\lambda_{\max}[\boldsymbol{X}]$ denotes the maximum eigenvalue of $\boldsymbol{X}$. As shown in (17), the SNIR_2 is a function of $\boldsymbol{t}_2 : \mathrm{SNIR}_2(\boldsymbol{t}_2) = \Gamma \cdot (\boldsymbol{t}_2^H\boldsymbol{H}^H\boldsymbol{H}\boldsymbol{t}_2)$. Thus, the optimization problem in (15) may be simplified to find $\boldsymbol{t}_2$ that can minimize the cost function

$$J(\boldsymbol{t}_2) = Q\left(\sqrt{\frac{3}{M-1}\mathrm{SNIR}_1(\boldsymbol{t}_2)}\right) + Q\left(\sqrt{\frac{3}{M-1}\mathrm{SNIR}_2(\boldsymbol{t}_2)}\right). \tag{20}$$

As shown in Appendix B, the optimum $\boldsymbol{t}_2$ that minimizes (20) lies within the range space of $\boldsymbol{H}^H\boldsymbol{H}$ and may be expressed as $\boldsymbol{t}_2 = \sqrt{q}\boldsymbol{v}_1 + \sqrt{1-q}\boldsymbol{v}_2$, where q is a real number within the interval $[0,1]$. With $\boldsymbol{t}_2 = \sqrt{q}\boldsymbol{v}_1 + \sqrt{1-q}\boldsymbol{v}_2$, the $\mathrm{SNIR}_1(\boldsymbol{t}_2)$ and $\mathrm{SNIR}_2(\boldsymbol{t}_2)$ may be expressed as a function of q in (21) and (22) at the bottom of the page (see Appendix B) where $\psi(q)$ in (21) is given as $\psi(q) = \Gamma/\{1+\Gamma\cdot(\lambda_1 q + \lambda_2(1-q))\}$. Since SNIR_1 and SNIR_2 are expressed in terms of q instead of $\boldsymbol{t}_2$, the cost function in (20) may be changed as

$$J(q) = Q\left(\sqrt{\frac{3}{M-1}\mathrm{SNIR}_1(q)}\right) + Q\left(\sqrt{\frac{3}{M-1}\mathrm{SNIR}_2(q)}\right). \tag{23}$$

We can show that the derivative of $J(q)$ may be expressed as $\partial J(q)/\partial q = f(q)\{g(q)-1\}$, where

$$f(q) = ((\sqrt{3}\Gamma(\lambda_1-\lambda_2))/(\sqrt{8\pi(M-1)})) \cdot \exp(-(3)/(2(M-1))\mathrm{SNIR}_2(q))/\sqrt{\mathrm{SNIR}_2(q)}$$

and

$$g(q) = \sqrt{((3)/(8\pi(M-1)))}((\partial \mathrm{SNIR}_1(q))/(\partial q)) \cdot \exp(-((3)/(2(M-1)))\mathrm{SNIR}_1(q))/\{f(q)\sqrt{\mathrm{SNIR}_1(q)}\}.$$

After some manipulations, we can show that $g(q)$ is an increasing function. In this case, since $f(q) > 0$, the derivative of $J(q)$ becomes zero for at most one q. Hence, $J(q)$ is a quasi-convex function [16]. To find q that minimizes $J(q)$, several numerical methods, such as Golden Section search or parabolic interpolation [18], may be used. Let the value of q that minimizes $J(q)$ be q_{opt}, and then the optimum $\boldsymbol{t}_2$ may be obtained as

$$\boldsymbol{t}_2^{(\mathrm{opt})} = \sqrt{q_{\mathrm{opt}}}\boldsymbol{v}_1 + \sqrt{1-q_{\mathrm{opt}}}\boldsymbol{v}_2. \tag{24}$$

From (18), the corresponding optimum $\boldsymbol{t}_1$ is given as

$$\boldsymbol{t}_1^{(\mathrm{opt})} = \boldsymbol{ev}_{\max}\left[\boldsymbol{A}\left(\boldsymbol{t}_2^{(\mathrm{opt})}\right)\right]. \tag{25}$$

The optimum receive weight vectors are obtained from (10) by replacing $\boldsymbol{t}_1$ and $\boldsymbol{t}_2$ with $\boldsymbol{t}_1^{(\mathrm{opt})}$ and $\boldsymbol{t}_2^{(\mathrm{opt})}$, respectively

$$\boldsymbol{r}_1^{(\mathrm{opt})} = \boldsymbol{\Phi}_1^{-1}\boldsymbol{H}\boldsymbol{t}_1^{(\mathrm{opt})} \tag{26}$$

$$\boldsymbol{r}_2^{(\mathrm{opt})} = \boldsymbol{\Phi}_2^{-1}\boldsymbol{H}\boldsymbol{t}_2^{(\mathrm{opt})} \tag{27}$$

where $\boldsymbol{t}_1$ and $\boldsymbol{t}_2$ in $\boldsymbol{\Phi}_1^{-1}$ and $\boldsymbol{\Phi}_2^{-1}$ should also be replaced with $\boldsymbol{t}_1^{(\mathrm{opt})}$ and $\boldsymbol{t}_2^{(\mathrm{opt})}$, respectively. When the optimum Tx and Rx filters given in (24)–(27) are applied, the corresponding SNIRs may be obtained from (21) and (22) by replacing q with q_{opt} : $\mathrm{SNIR}_1(q_{\mathrm{opt}})$ and $\mathrm{SNIR}_2(q_{\mathrm{opt}})$.

IV. Proposed Transmit and Receive Filters

In this section, we extend the results of Section III-B to the case where the number of data symbols K is more than two. A Tx and Rx filters design criterion, referred to as *equal SNIR criterion*, is derived in Section IV-A, and the proposed Tx and Rx filters based on this equal SNIR criterion are described in Section IV-B. The BEP performance of the proposed filter is analyzed and compared with that of MMSE filter in Section IV-C.

A. Tx and Rx Filters Design Criterion: Equal SNIR Criterion

In this subsection, we investigate the asymptotic behavior of SNIR_k in (11) as TxSNR becomes high, and derive a Tx and Rx filters design criterion. For high TxSNR, Γ, $\boldsymbol{\Phi}_k^{-1}$ in (12) may be approximated as

$$\begin{aligned}\boldsymbol{\Phi}_k^{-1} &= \Gamma\boldsymbol{I}_{N_R} - \sum_{i=k+1}^{K}\frac{\boldsymbol{\Phi}_i^{-1}\boldsymbol{H}\boldsymbol{t}_i\boldsymbol{t}_i^H\boldsymbol{H}^H\boldsymbol{\Phi}_i^{-1}}{1+\boldsymbol{t}_i^H\boldsymbol{H}^H\boldsymbol{\Phi}_i^{-1}\boldsymbol{H}\boldsymbol{t}_i} \\ &\cong \Gamma\boldsymbol{I}_{N_R} - \sum_{i=k+1}^{K}\frac{\boldsymbol{\Phi}_i^{-1}\boldsymbol{H}\boldsymbol{t}_i\boldsymbol{t}_i^H\boldsymbol{H}^H\boldsymbol{\Phi}_i^{-1}}{\boldsymbol{t}_i^H\boldsymbol{H}^H\boldsymbol{\Phi}_i^{-1}\boldsymbol{H}\boldsymbol{t}_i}.\end{aligned} \tag{28}$$

With this approximated $\boldsymbol{\Phi}_k^{-1}$, the SNIR_k in (11) may be approximated as

$$\begin{aligned}\mathrm{SNIR}_k &= \boldsymbol{t}_k^H\boldsymbol{H}^H\boldsymbol{\Phi}_k^{-1}\boldsymbol{H}\boldsymbol{t}_k \\ &\cong \Gamma\left(\boldsymbol{t}_k^H\boldsymbol{H}^H\boldsymbol{H}\boldsymbol{t}_k\right) - \sum_{i=k+1}^{K}\frac{\left|\boldsymbol{t}_k^H\boldsymbol{H}^H\boldsymbol{\Phi}_i^{-1}\boldsymbol{H}\boldsymbol{t}_i\right|^2}{\boldsymbol{t}_i^H\boldsymbol{H}^H\boldsymbol{\Phi}_i^{-1}\boldsymbol{H}\boldsymbol{t}_i}.\end{aligned} \tag{29}$$

$$\begin{aligned}\mathrm{SNIR}_1(q) = \frac{\Gamma}{2}\Big\{&\left(\lambda_1+\lambda_2-\psi(q)\cdot\left(\lambda_1^2 q+\lambda_2^2(1-q)\right)\right) \\ &+\sqrt{\left(\lambda_1+\lambda_2-\psi(q)\cdot(\lambda_1^2 q+\lambda_2^2(1-q))\right)^2 - 4\lambda_1\lambda_2(1-\psi(q)\cdot(\lambda_1 q+\lambda_2(1-q)))}\Big\}\end{aligned} \tag{21}$$

$$\mathrm{SNIR}_2(q) = \Gamma\cdot(\lambda_1 q + \lambda_2(1-q)) \tag{22}$$

Moreover, the product of these approximated SNIR_k's may be expressed as (see Appendix C)

$$\prod_{k=1}^{K} \mathrm{SNIR}_k = \Gamma^K \cdot \det[\boldsymbol{T}^H \boldsymbol{H}^H \boldsymbol{H}\boldsymbol{T}]. \quad (30)$$

where $\det[\boldsymbol{X}]$ denotes the determinant of a matrix $\boldsymbol{X}$. Using the Hadamard's inequality [17], we can show that

$$\det[\boldsymbol{T}^H \boldsymbol{H}^H \boldsymbol{H}\boldsymbol{T}] \leq \prod_{k=1}^{K} \boldsymbol{t}_k^H \boldsymbol{H}^H \boldsymbol{H}\boldsymbol{t}_k$$

where $\boldsymbol{t}_k^H \boldsymbol{H}^H \boldsymbol{H}\boldsymbol{t}_k$ is the kth diagonal element of $\boldsymbol{T}^H \boldsymbol{H}^H \boldsymbol{H}\boldsymbol{T}$, and equality holds if and only if the off-diagonal elements $\boldsymbol{t}_i^H \boldsymbol{H}^H \boldsymbol{H}\boldsymbol{t}_j = 0, i \neq j$, are zero. One example of $\boldsymbol{T}$ that makes $\boldsymbol{t}_i^H \boldsymbol{H}^H \boldsymbol{H}\boldsymbol{t}_j = 0$ for $i \neq j$ is $\boldsymbol{T} = \boldsymbol{V}$, with which the diagonal element $\boldsymbol{t}_k^H \boldsymbol{H}^H \boldsymbol{H}\boldsymbol{t}_k$ becomes λ_k. Thus, it holds that

$$\det[\boldsymbol{T}^H \boldsymbol{H}^H \boldsymbol{H}\boldsymbol{T}] \leq \prod_{k=1}^{K} \lambda_k.$$

Consequently, the product of all SNIR_k's in (29) may be upper-bounded as

$$\prod_{k=1}^{K} \mathrm{SNIR}_k \leq \Gamma^K \cdot \prod_{k=1}^{K} \lambda_k. \quad (31)$$

In this case, the BEP cost function $J(\boldsymbol{t}_1, \boldsymbol{t}_2, \ldots, \boldsymbol{t}_K)$ in (13) is minimized when the product of SNIR_k's equals $\Gamma^K \cdot \prod_{k=1}^{K} \lambda_k$, and all the SNIR_k's are the same (see Appendix D). Thus, it is desirable to design Tx and Rx filters with which the product of SNIR_k's approaches to the value of $\Gamma^K \cdot \prod_{k=1}^{K} \lambda_k$, and all the SNIR_k's are as close to one another as possible. We refer to this design criterion as the *equal SNIR criterion*.

B. Proposed Tx and Rx Filters Based on the Equal SNIR Criterion

In this subsection, based on the equal SNIR criterion, we propose Tx and Rx filters for an arbitrary number of data symbols K. Since the Rx filter can be obtained from (10) after finding a Tx filter, we concentrate on designing the Tx filter. For the case of $K = 2$, we can show that two optimum Tx weight vectors given in (24) and (25) lie on the two-dimensional (2-D) range space of $\boldsymbol{H}^H \boldsymbol{H}$. Similarly, for the general case of K, if two Tx weight vectors $\boldsymbol{t}_k$ and $\boldsymbol{t}_{k'}$ are forced to lie in a 2-D range *subspace* of $\boldsymbol{H}^H \boldsymbol{H}$, then we may obtain $\boldsymbol{t}_k$ and $\boldsymbol{t}_{k'}$ optimized within the 2-D range subspace. According to the equal SNIR criterion, the condition

$$\prod_{k=1}^{K} \mathrm{SNIR}_k \cong \Gamma^K \cdot \prod_{k=1}^{K} \lambda_k$$

should be satisfied for high TxSNR. To satisfy this condition, we propose that the pairs of two Tx weight vectors lie in *the nonoverlapping 2-D range subspaces* of $\boldsymbol{H}^H \boldsymbol{H}$ where "nonoverlapping" means that any two 2-D range subspaces do not share the same basis $\boldsymbol{v}_k$. For the case of an odd K, the remaining one Tx weight is proposed to lie in the remaining one-dimensional range subspace of $\boldsymbol{H}^H \boldsymbol{H}$. Let us denote the 2-D range subspace of $\boldsymbol{H}^H \boldsymbol{H}$ spanned by $\boldsymbol{v}_i$ and $\boldsymbol{v}_j$ as $\boldsymbol{s}_{i,j}$, and assume that $\boldsymbol{t}_k$ and $\boldsymbol{t}_{k'}$ are forced to lie and optimized in $\boldsymbol{s}_{i,j}$. Then, as shown in Section IV-C, the corresponding SNIR_k and $\mathrm{SNIR}_{k'}$ may be expressed for high TxSNR as $\mathrm{SNIR}_k \cong \mathrm{SNIR}_{k'} \cong \Gamma\sqrt{\lambda_i \lambda_j}$. Note that SNIR_k and $\mathrm{SNIR}_{k'}$ are determined by two eigenvalues λ_i and λ_j associated with $\boldsymbol{v}_i$ and $\boldsymbol{v}_j$ for $\boldsymbol{s}_{i,j}$. Moreover, since the pairs of two Tx weight vectors are proposed to lie in the *nonoverlapping* 2-D range subspaces, the pairs of two SNIRs are determined by the distinct pairs of two eigenvalues. Hence, the product of SNIRs may be expressed for high TxSNR as

$$\prod_{k=1}^{K} \mathrm{SNIR}_k \cong \Gamma^K \cdot \prod_{k=1}^{K} \lambda_k.$$

Note that the pair of two SNIRs become identical, but different pairs of SNIRs are different from each other due to the distinct pairs of two eigenvalues. According to the equal SNIR criterion, it is desirable to make all the SNIRs as close to one another as possible. Thus, two eigenvalues for the pairs of two SNIRs should be chosen in such a way that the largest eigenvalue is paired with the smallest one and the second largest eigenvalue with the second smallest one, and so on. Hence, we propose the use of $\boldsymbol{s}_{1+m,K-m}, m = 0, 1, \ldots, \lfloor (K-2)/2 \rfloor$ for the nonoverlapping 2-D range subspaces, since the $(m+1)$th largest eigenvalue is paired with the $(m+1)$th smallest one using $\boldsymbol{s}_{1+m,K-m}$.[1] Although any pair of two Tx weights vector may be forced to lie in $\boldsymbol{s}_{1+m,K-m}$, for notational simplicity, we choose $\boldsymbol{t}_{1+m}$ and $\boldsymbol{t}_{K-m}, m = 0, 1, \ldots, \lfloor (K-2)/2 \rfloor$ for the pair of two Tx weight vectors that lie in $\boldsymbol{s}_{1+m,K-m}$. For the case of an odd K, the remaining one Tx weight $\boldsymbol{t}_{(K+1)/2}$ is proposed to lie in the remaining one-dimensional range subspace of $\boldsymbol{H}^H \boldsymbol{H}$ spanned by $\boldsymbol{v}_{(K+1)/2}$. In this case, $\boldsymbol{t}_{(K+1)/2} = \boldsymbol{v}_{(K+1)/2}$, and no optimization is needed for $\boldsymbol{t}_{(K+1)/2}$.

Now we derive the proposed Tx and Rx filters based on the assumption that $\boldsymbol{t}_{1+m}$ and $\boldsymbol{t}_{K-m}$ lie in $\boldsymbol{s}_{1+m,K-m}$. As shown in Appendix E, two SNIRs corresponding to $\boldsymbol{t}_{1+m}$ and $\boldsymbol{t}_{K-m}$ may be expressed as

$$\mathrm{SNIR}_{1+m} = \Gamma \cdot \left(\boldsymbol{t}_{1+m}^H \boldsymbol{H}^H \boldsymbol{H}\boldsymbol{t}_{1+m}\right) - \frac{\Gamma^2 \cdot \left|\boldsymbol{t}_{1+m}^H \boldsymbol{H}^H \boldsymbol{H}\boldsymbol{t}_{K-m}\right|^2}{1 + \Gamma \cdot \left(\boldsymbol{t}_{K-m}^H \boldsymbol{H}^H \boldsymbol{H}\boldsymbol{t}_{K-m}\right)} \quad (32)$$

$$\mathrm{SNIR}_{K-m} = \Gamma \cdot \left(\boldsymbol{t}_{K-m}^H \boldsymbol{H}^H \boldsymbol{H}\boldsymbol{t}_{K-m}\right). \quad (33)$$

Moreover, since $\boldsymbol{t}_{1+m}$ and $\boldsymbol{t}_{K-m}$ lie in $\boldsymbol{s}_{1+m,K-m}$, SNIR_{1+m} and SNIR_{K-m} are further simplified to

$$\mathrm{SNIR}_{1+m} = \Gamma \cdot \left(\boldsymbol{t}_{1+m}^H \boldsymbol{H}_m^H \boldsymbol{H}_m \boldsymbol{t}_{1+m}\right) - \frac{\Gamma^2 \cdot \left(\boldsymbol{t}_{1+m}^H \boldsymbol{H}_m^H \boldsymbol{H}_m \boldsymbol{t}_{K-m} \boldsymbol{t}_{K-m}^H \boldsymbol{H}_m^H \boldsymbol{H}_m \boldsymbol{t}_{1+m}\right)}{1 + \Gamma \cdot \left(\boldsymbol{t}_{K-m}^H \boldsymbol{H}_m^H \boldsymbol{H}_m \boldsymbol{t}_{K-m}\right)} \quad (34)$$

$$\mathrm{SNIR}_{K-m} = \Gamma \cdot \left(\boldsymbol{t}_{K-m}^H \boldsymbol{H}_m^H \boldsymbol{H}_m \boldsymbol{t}_{K-m}\right) \quad (35)$$

where $\boldsymbol{H}_m$ is a projection of $\boldsymbol{H}$ onto $\boldsymbol{s}_{1+m,K-m}$

$$\boldsymbol{H}_m^H \boldsymbol{H}_m = [\boldsymbol{v}_{1+m} \; \boldsymbol{v}_{K-m}] \begin{bmatrix} \lambda_{1+m} & 0 \\ 0 & \lambda_{K-m} \end{bmatrix} \begin{bmatrix} \boldsymbol{v}_{1+m}^H \\ \boldsymbol{v}_{K-m}^H \end{bmatrix}. \quad (36)$$

[1]Note that $\boldsymbol{s}_{1+m,K-m}$ is spanned by $\boldsymbol{v}_{1+m}$ and $\boldsymbol{v}_{K-m}$, which are associated with the $(m+1)$th largest and the $(m+1)$th smallest eigenvalues, respectively.

Note that SNIR_{1+m} and SNIR_{K-m} are determined by only two Tx weight vectors $\boldsymbol{t}_{1+m}$ and $\boldsymbol{t}_{K-m}$. This indicates that the interference caused by the symbols whose Tx weights vectors lie in the different 2-D subspaces becomes zero. Consequently, the cost function $J(\boldsymbol{t}_1, \boldsymbol{t}_2, \ldots, \boldsymbol{t}_K)$ in (13) may be simplified as

$$J(\boldsymbol{t}_1, \boldsymbol{t}_2, \ldots, \boldsymbol{t}_K) = \sum_{m=0}^{\lfloor (K-2)/2 \rfloor} J(\boldsymbol{t}_{1+m}, \boldsymbol{t}_{K-m})$$

where $J(\boldsymbol{t}_{1+m}, \boldsymbol{t}_{K-m})$ is given as

$$J(\boldsymbol{t}_{1+m}, \boldsymbol{t}_{K-m}) = Q\left(\sqrt{\frac{3}{M-1}\text{SNIR}_{1+m}}\right) + Q\left(\sqrt{\frac{3}{M-1}\text{SNIR}_{K-m}}\right). \quad (37)$$

Moreover, the minimization of the cost function $J(\boldsymbol{t}_1, \boldsymbol{t}_2, \ldots, \boldsymbol{t}_K)$ may be accomplished by separately minimizing the cost functions $J(\boldsymbol{t}_{1+m}, \boldsymbol{t}_{K-m})$'s. Observe the similarity between (37) and (15). Hence, following the procedure in Section III-B, we may obtain the proposed Tx weight vectors as

$$\boldsymbol{t}_{K-m} = \sqrt{q_m^{(\text{opt})}}\boldsymbol{v}_{1+m} + \sqrt{1 - q_m^{(\text{opt})}}\boldsymbol{v}_{K-m} \quad (38)$$

$$\boldsymbol{t}_{1+m} = \boldsymbol{ev}_{\max}\left[\boldsymbol{A}_m\left(\boldsymbol{t}_{K-m}^{(\text{opt})}\right)\right] \quad (39)$$

where $q_m^{(\text{opt})}$ in (38) denotes q that minimizes (23) when λ_1 and λ_2 in $\text{SNIR}_1(q)$ and $\text{SNIR}_2(q)$ are replaced with λ_{1+m} and λ_{K-m}, respectively. Similarly, with $\boldsymbol{A}(\boldsymbol{x})$ in (19), $\boldsymbol{A}_m(\boldsymbol{x})$ in (39) is defined as

$$\boldsymbol{A}_m(\boldsymbol{x}) \triangleq \boldsymbol{H}_m^H\boldsymbol{H}_m - \frac{\Gamma \cdot \left(\boldsymbol{H}_m^H\boldsymbol{H}_m\boldsymbol{x}\boldsymbol{x}^H\boldsymbol{H}_m^H\boldsymbol{H}_m\right)}{1 + \Gamma \cdot \left(\boldsymbol{x}^H\boldsymbol{H}_m^H\boldsymbol{H}_m\boldsymbol{x}\right)}. \quad (40)$$

With the proposed Tx weight vectors given in (38) and (39), the corresponding Rx weight vectors may be obtained from (10). Note that, when $K = 2$, the proposed Tx and Rx weights vectors become the optimum Tx and Rx weight vectors given in (24)–(27).

C. Performance of the Proposed Filter and Comparison With That of the MMSE Filter

In this subsection, the BEP performance of the proposed filter is analyzed and compared with that of MMSE filter. Similarly to the case of $K = 2$, when the proposed Tx and Rx filters are applied, the corresponding SNIRs may be obtained as shown in (41) and (42) at the bottom of the page, where $\psi_m(x)$ in (41) is given as $\psi_m(x) = \Gamma/\{1 + \Gamma \cdot (\lambda_{1+m}x + \lambda_{K-m}(1-x))\}$. For an odd K, the remaining SNIR $\text{SNIR}_{(K+1)/2}$ may be expressed as $\text{SNIR}_{(K+1)/2} = \Gamma\lambda_{(K+1)/2}$. With these SNIRs, the overall BEP of the proposed filter may be obtained from (7). The average BEP (ABEP) may be obtained by averaging this BEP over the channel matrix $\boldsymbol{H}$

$$\text{ABEP} = E[\text{BEP}] \cong E\left[\frac{4 \cdot (1 - 1/\sqrt{M})}{K \cdot \log_2 M}\sum_{k=1}^{K} Q\left(\sqrt{\frac{3}{M-1}\text{SNIR}_k}\right)\right]. \quad (43)$$

Now let us consider the performance of the MMSE filter given in [9]. The MMSE filter decouples the MIMO channel $\boldsymbol{H}$ into K parallel eigen-subchannels, and allocate the total Tx power $K \cdot P$ on these subchannels according to the inverse-water-pouring policy [9]. The SNIRs with the MMSE filter can be expressed as [9]

$$\text{SNIR}_k^{(\text{MMSE})} = \left(\Gamma\frac{K\sqrt{\lambda_k}}{\sum_{i=1}^{K}\lambda_i^{-\frac{1}{2}}} + \frac{\sqrt{\lambda_k}\sum_{i=1}^{K}\lambda_i^{-1}}{\sum_{i=1}^{K}\lambda_i^{-\frac{1}{2}}} - 1\right)_+, \quad k = 1, 2, \ldots, K \quad (44)$$

where $(x)_+$ denotes $\max(x, 0)$. The ABEP of the MMSE filter may be obtained from (43) by substituting SNIR_k with $\text{SNIR}_k^{(\text{MMSE})}$ in (44).

Similarly to the case of $K = 2$ (see Appendix F), when the proposed filter given in (41) and (42) is used, the SNIRs may be expressed for high TxSNR as

$$\text{SNIR}_{1+m} \cong \text{SNIR}_{K-m} \cong \Gamma\sqrt{\lambda_{1+m}\lambda_{K-m}}.$$

Whereas, from (44), the SNIRs with the MMSE filter may be expressed as

$$\text{SNIR}_k^{(\text{MMSE})} \cong \Gamma K\sqrt{\lambda_k}/\sum_{i=1}^{K}\lambda_i^{-(1/2)}$$

for high TxSNR. To compare the BEP performance of the proposed filter with that of the MMSE filter, consider the following two cases of eigenvalues:

i) all eigenvalues are equal;
ii) the smallest eigenvalue λ_K is much smaller than the others.

The first case is observed when the number of Tx antennas is much larger or smaller than that of Rx antennas, and the second case when the numbers of Tx and Rx antennas are the same. In case i), the SNIRs with the proposed filter may be expressed as $\text{SNIR}_k \cong \Gamma\lambda_k$, and those with the MMSE filter may be simplified as $\text{SNIR}_k^{(\text{MMSE})} \cong \Gamma\lambda_k$. Note that the SNIRs with the proposed filter are the same as those with the MMSE filter. Hence, in case i), the performance of the proposed filter becomes the

$$\text{SNIR}_{1+m} = \frac{\Gamma}{2}\left\{\left(\lambda_{1+m} + \lambda_{K-m} - \psi_m\left(q_m^{(\text{opt})}\right)\left(\lambda_{1+m}^2 q_m^{(\text{opt})} + \lambda_{K-m}^2\left(1 - q_m^{(\text{opt})}\right)\right)\right) + \sqrt{\begin{array}{l}\left(\lambda_{1+m} + \lambda_{K-m} - \psi_m\left(q_m^{(\text{opt})}\right)\left(\lambda_{1+m}^2 q_m^{(\text{opt})} + \lambda_{K-m}^2\left(1 - q_m^{(\text{opt})}\right)\right)\right)^2 \\ -4\lambda_{1+m}\lambda_{K-m}\left(1 - \psi_m\left(q_m^{(\text{opt})}\right)\left(\lambda_{1+m}q_m^{(\text{opt})} + \lambda_{K-m}\left(1 - q_m^{(\text{opt})}\right)\right)\right)\end{array}}\right\} \quad (41)$$

$$\text{SNIR}_{K-m} = \Gamma \cdot \left(\lambda_{1+m}q_m^{(\text{opt})} + \lambda_{K-m}\left(1 - q_m^{(\text{opt})}\right)\right), \qquad m = 0, 1, \ldots, \lfloor (K-2)/2 \rfloor \quad (42)$$

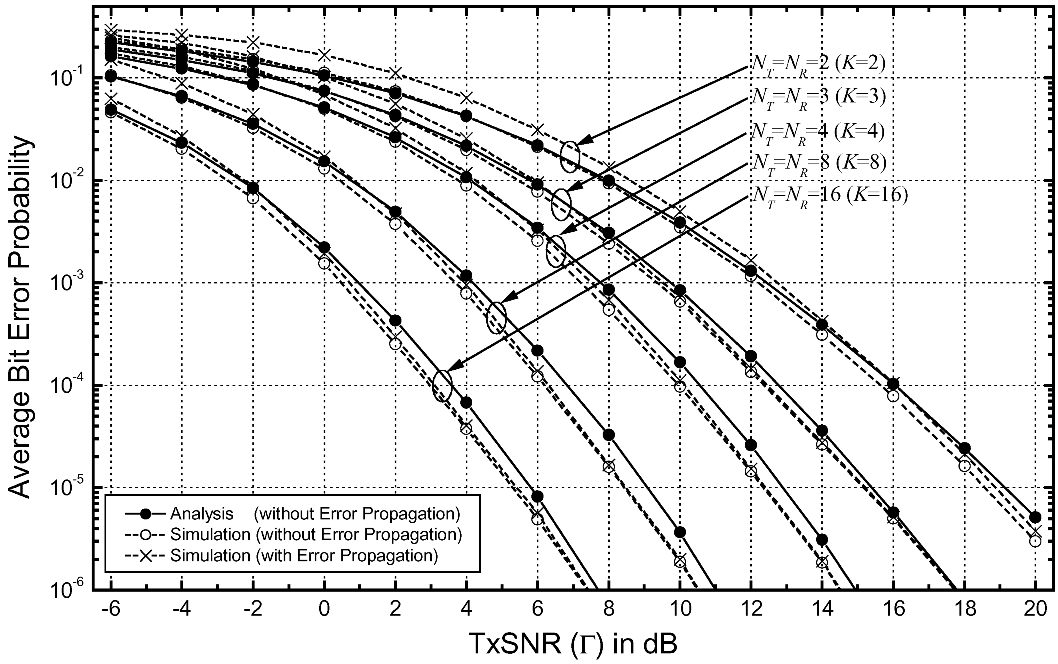

Fig. 2. ABEP of the proposed filter for various N_T and N_R.

same as that of the MMSE filter. In case ii), the SNIRs with the MMSE filter can be approximated as

$$\text{SNIR}_k^{(\text{MMSE})} \cong \Gamma K \sqrt{\lambda_k \lambda_K}.$$

We can see that the smallest eigenvalue λ_K affects all the SNIRs, and $\text{SNIR}_K^{(\text{MMSE})}$ becomes much smaller than the others. Hence, the performance of the MMSE filter is limited by $\text{SNIR}_K^{(\text{MMSE})}$. Moreover, regardless of K, the distribution of $\text{SNIR}_K^{(\text{MMSE})} \cong \Gamma K \lambda_K$ is known to follow the chi-square distribution with two degrees of freedom [19]. Hence, in case ii), the diversity order of the MMSE filter becomes one regardless of K [12]. Whereas, the proposed filter compensates the $(m+1)$th smallest eigenvalue λ_{K-m} with the $(m+1)$th largest eigenvalue λ_{1+m}. Hence, the performance of the proposed filter may not be limited by the smallest eigenvalue.

V. Numerical Results

In this section, based on (43), we present the BEP performance of the proposed filter. For comparison, we also present the BEP performance of the MMSE filter. All the results shown in this section are obtained analytically through Monte Carlo integration [18] based on 10^6 independent realizations of the channel matrix $\boldsymbol{H}$. Since ABEP when $(N_T, N_R) = (a, b)$ is the same as that when $(N_T, N_R) = (b, a)$,[2] we consider only the case of $N_T \geq N_R$, in which the number of data symbols K is equal to N_R. Moreover, we consider only 4-QAM ($M = 4$).

Fig. 2 shows the analysis and simulation results of the proposed filter for various N_T and N_R. Analysis is performed without error propagation, whereas simulation is performed both with and without error propagation. Comparing the simulation results with and without error propagation, we can see that the effects of error propagation are negligible for the proposed filter. The reason is that when the proposed filter is applied, only two symbols whose Tx weight vectors lie in the same 2-D subspace interfere with each other. Hence, when canceling the previously decided symbols, at most one data symbol affects the current symbol decision. Comparing the analysis and simulation results without error propagation, the analysis and simulation results show a close agreement even though the Gaussian approximation is used for approximating interference in analysis. This indicates that the Gaussian approximation used in analysis is quite accurate even when K is small.

Fig. 3 shows the BEP performance of the proposed and MMSE filters when $N_T = 2$ and $N_R = 2$. Note that in this case ($K = 2$), the performance of the proposed filter becomes the same with that of the optimum filter. In this figure, "ABEP_k" denotes the ABEP for the kth data symbol d_k. Note that for the MMSE filter, the ABEP_2 is much worse than ABEP_1, and dominates the ABEP. The reason is that $\text{SNIR}_2^{(\text{MMSE})}$ is much smaller than $\text{SNIR}_1^{(\text{MMSE})}$ due to the smallest eigenvalue. Unlike the MMSE filter, two SNIRs with the proposed filter become the same for high TxSNR: $\text{SNIR}_1 \cong \text{SNIR}_2$ (see Appendix F). Thus, for the proposed filter, the ABEP_1 becomes the same as the ABEP_2 as TxSNR increases. Consequently, the proposed filter is observed to significantly outperform the MMSE filter in ABEP. Fig. 4 depicts the ABEPs of the proposed filter and the MMSE filter when $N_T = 4$ and $N_R = 4$. Like in Fig. 3, this figure shows that the proposed filter outperforms the MMSE filter in ABEP. Note that the ABEP of the MMSE filter is limited by ABEP_4, which is associated with the smallest SNIR. Note also that since the proposed filter is optimized in $\boldsymbol{s}_{1+m,K-m}$ ($\boldsymbol{s}_{1,4}$ and $\boldsymbol{s}_{2,3}$), ABEP_1 is almost the same as ABEP_4, as in ABEP_2 and ABEP_3. A slight difference between the pair ABEP_1, ABEP_4 and ABEP_2, ABEP_3 is due to the inherent differences in the eigenvalues.

Figs. 5 and 6 show the effects of N_T on the BEP performance of the proposed and the MMSE filters when N_R is fixed at 2. Fig. 5(a) and (b), respectively, depicts the mean and variance of

[2]This is due to the fact that $\boldsymbol{H}^H\boldsymbol{H}$ and $\boldsymbol{H}\boldsymbol{H}^H$ have the same eigenvalues, which determine the SNIRs in (41) and (42).

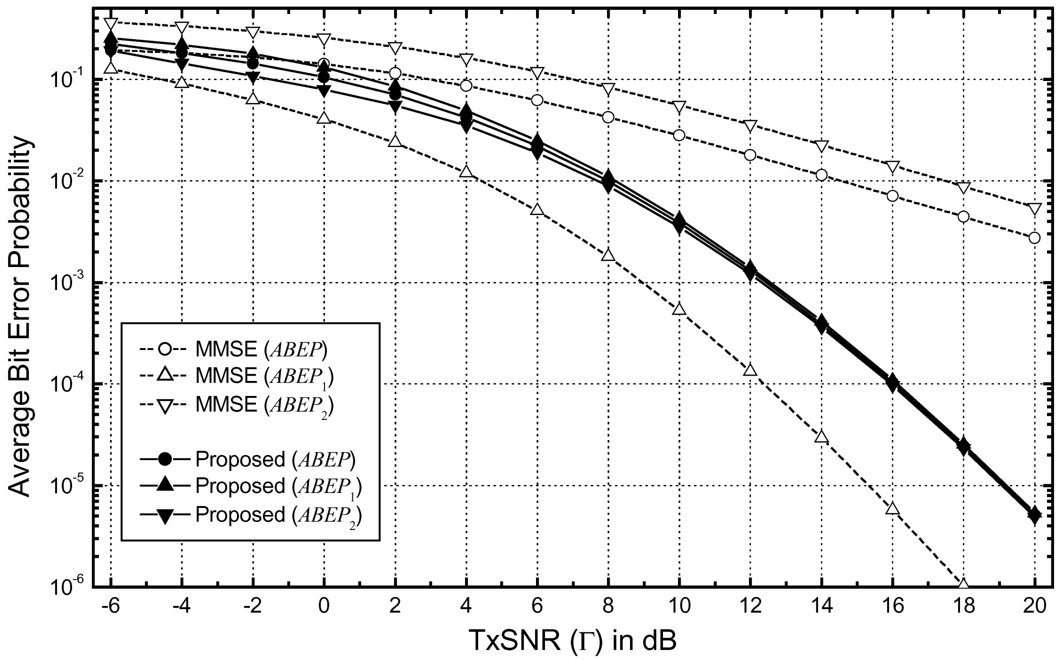

Fig. 3. ABEP of the proposed and the MMSE filters when $N_T = 2$ and $N_R = 2\,(K = 2)$.

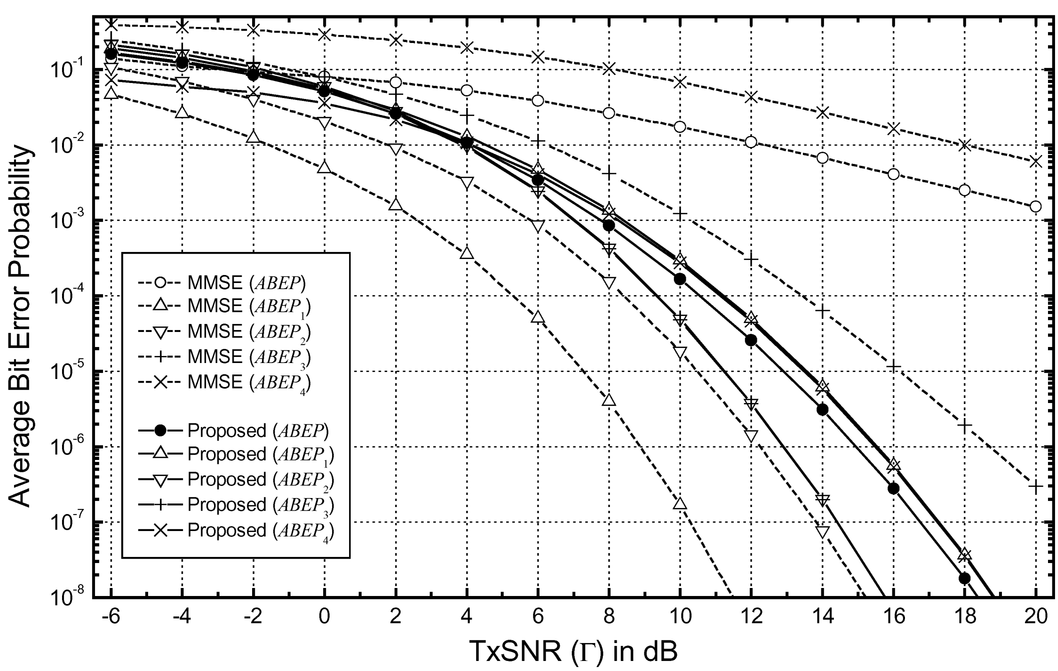

Fig. 4. ABP of the proposed and the MMSE filters when $N_T = 4$ and $N_R = 4\,(K = 4)$.

SNIRdB_k when $\Gamma = 10$ dB where SNIRdB_k is defined as $\mathrm{SNIRdB}_k \triangleq 10\log(\mathrm{SNIR}_k^{(\mathrm{MMSE})})$ for the MMSE filter and $\mathrm{SNIRdB}_k \triangleq 10\log(\mathrm{SNIR}_k)$ for the proposed filter. Note that for the MMSE filter, the means of SNIRdB_1 and SNIRdB_2 increase to about 3 dB as N_T doubles, and the variances decrease and approach zero as N_T increases. This increase in mean and decrease in variance may be interpreted as "*beamforming gain*" and "*diversity gain*," respectively. Similar to the MMSE filter, the proposed filter also provides this beamforming gain and diversity gain. Fig. 6 depicts the ABEPs of the proposed and MMSE filters for various N_T. As N_T increases, the slopes of ABEP curves for both the proposed and MMSE filters become steeper due to the increase in diversity gain. As N_T doubles, the ABEP curves for both the proposed and the MMSE filters shift toward the left more than 3 dB due to the increases in beamforming and diversity gains. These observations confirm that both the proposed and the MMSE filters provide both beamforming and diversity gains when N_T increases for a fixed N_R. Note that the proposed filter provides a significant improvement in performance over the MMSE filter when N_T is small, and the performance improvement decreases as N_T increases. For example, the proposed filter provides 6.0 dB of

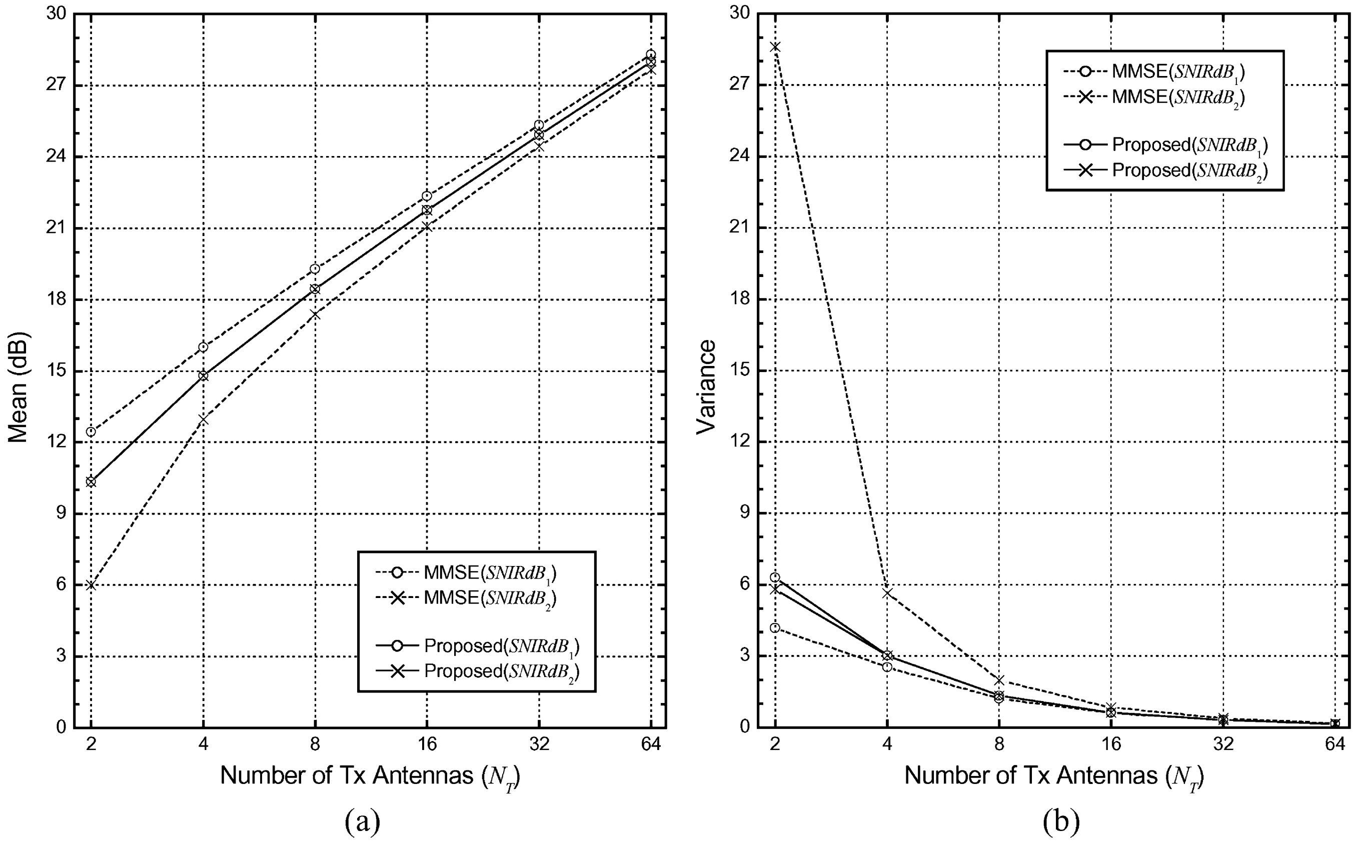

Fig. 5. Mean and variance of $\text{SNIRdB}_k \triangleq 10\log(\text{SNIR}_k)$ for various N_T when $\Gamma = 10$ dB and $N_R = 2\,(K = 2)$: (a) mean and (b) variance.

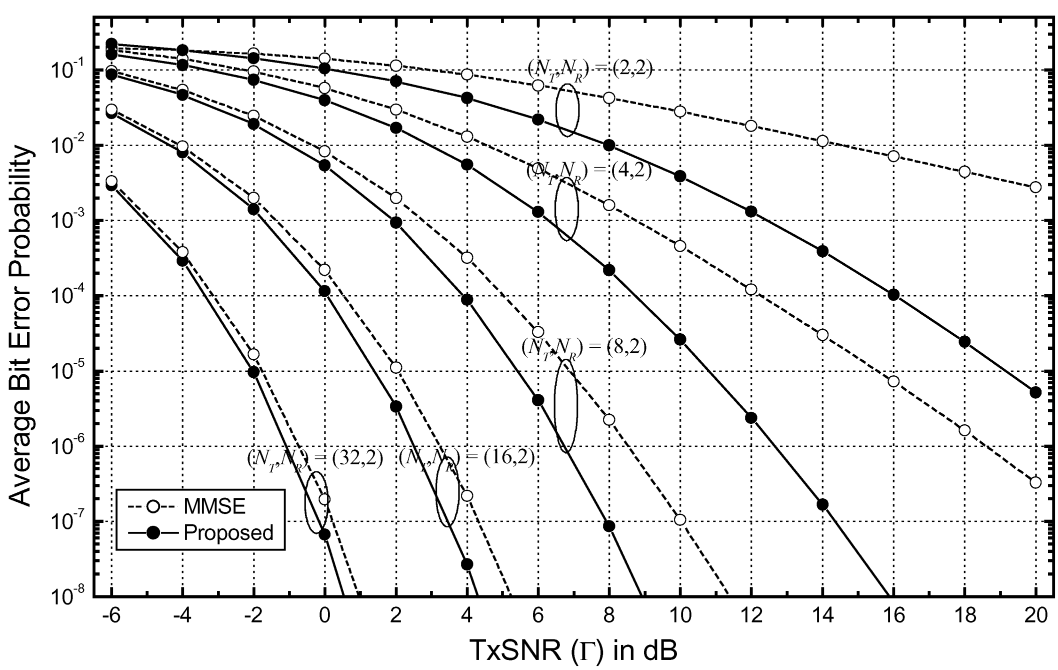

Fig. 6. ABEP of the proposed and the MMSE filters for various N_T when $N_R = 2\,(K = 2)$.

TxSNR gain over the MMSE filter at ABEP of 10^{-6} when $N_T = 4$, and 1.8-dB gain when $N_T = 8$. The reason is that, as mentioned in Section IV-C, all eigenvalues of $\boldsymbol{H}^H\boldsymbol{H}$ become the same as N_T increases for a fixed N_R.

Fig. 7 shows the effects of N_T and N_R on the BEP performance of the proposed and the MMSE filters when $N_T = N_R$. Note that the performance of the proposed filter is significantly improved as both N_T and N_R increase, whereas, the performance improvement of the MMSE filter is not as significant as that of the proposed filter. Especially, the slopes of ABEP curves for the MMSE filter remain constant regardless of N_T and N_R. The reason is that, as mentioned in Section IV-C, the diversity

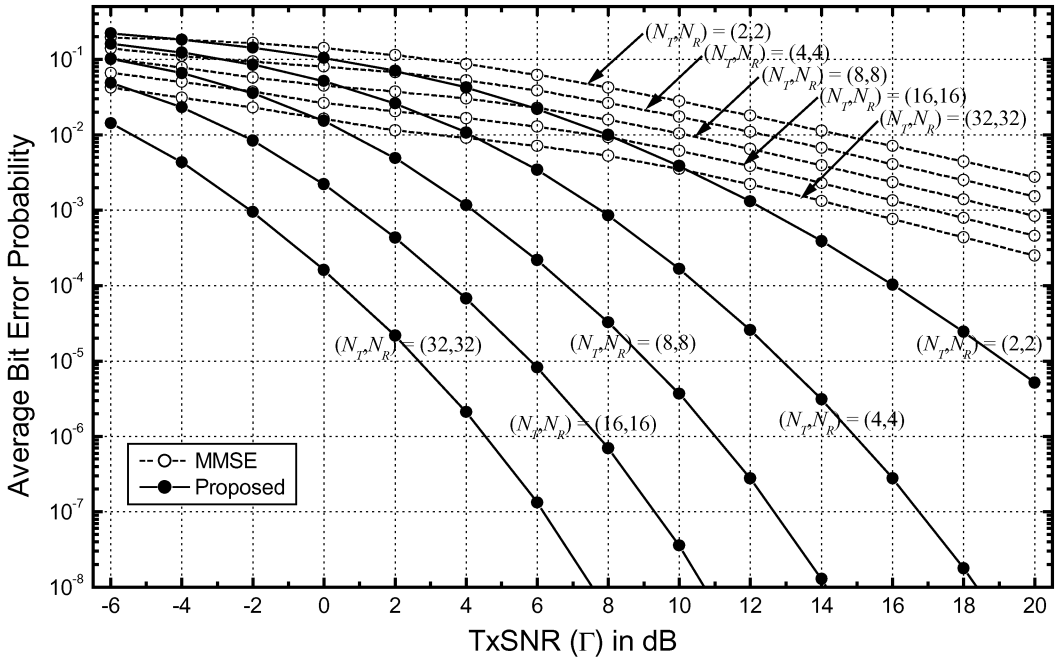

Fig. 7. ABEP of the proposed and the MMSE filters for various N_T and N_R when $N_T = N_R\,(K = N_R)$.

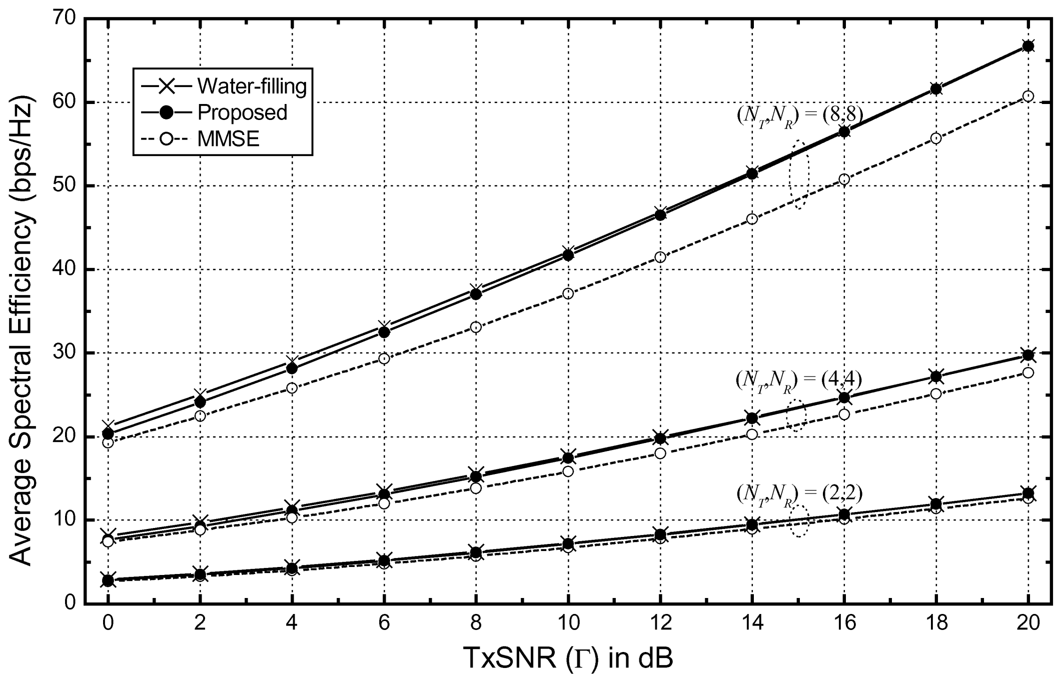

Fig. 8. Average SE of the proposed and the MMSE filters for various N_T and N_R when $N_T = N_R(K = N_R)$.

order of the MMSE filter becomes one when $N_T = N_R$. Consequently, as both N_T and N_R increase, the proposed filter provides a significant improvement in BEP over the MMSE filter.

VI. Discussion

Along with the BEP, the spectral efficiency (SE) is another performance measure of the MIMO system. In this section, we discuss the SE of the MIMO system with the proposed filter. Also, we investigate the effect of imperfect CSI at the transmitter on the BEP performance.

A. Spectral Efficiency (SE)

As discussed in Section V, the interference in (6) may be approximated as a Gaussian random variable. In this case, the SE of the MIMO system with the proposed filter may be approximated as [20]

$$\mathrm{SE} \cong \sum_{k=1}^{K} \log_2(1 + \mathrm{SNIR}_k). \tag{45}$$

In Fig. 8, the average spectral efficiency of the proposed filter, defined as $\mathrm{ASE} = E[\mathrm{SE}]$, is shown and compared with that of the MMSE filter. The water-filling capacity [21], also plotted

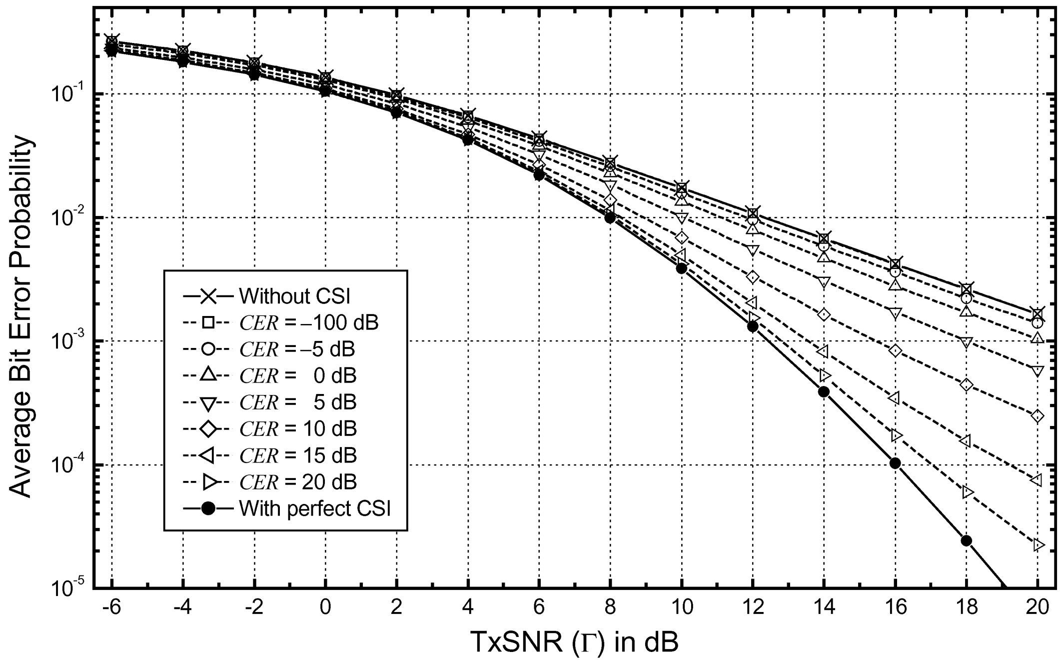

Fig. 9. ABEP of the proposed filter for various CER when $N_T = 2$ and $N_R = 2\,(K = 2)$.

in Fig. 8, represents an upper bound on the SE attainable with the MIMO system. Note that the SE of the proposed filter is higher than that of the MMSE filter, and the difference becomes larger as the number of antennas increases. Note also that even though the proposed filter is designed to minimize the BEP performance, the SE of the proposed filter converges to the optimum water-filling capacity when the TxSNR increases. The reason is that when the TxSNR increases, the SE of the proposed filter may be approximated as

$$\mathrm{SE} \cong \sum_{k=1}^{K} \log_2(\mathrm{SNIR}_k) \cong \log_2(\Gamma^K \prod_{k=1}^{K} \lambda_k)$$

which corresponds to the approximated water-filling capacity at high TxSNR [21].

B. Effect of Imperfect CSI at the Transmitter

The proposed filter in Section IV assumes that the CSI at the transmitter is perfect. In practical systems, however, the CSI may be noisy and outdated due to the channel estimation error and time-varying channel. In this subsection, we discuss the effect of imperfect CSI at the transmitter on the BEP performance. We model the imperfect CSI at the transmitter as

$$\hat{\boldsymbol{H}} = \boldsymbol{H} + \boldsymbol{E} \tag{46}$$

where $\boldsymbol{E}$ denotes an $N_R \times N_T$ error matrix, whose elements are i.i.d. zero-mean circular complex AWGN with the variance of σ_E^2. We assume that the proposed Tx filter is derived with $\hat{\boldsymbol{H}}$ instead of $\boldsymbol{H}$. Fig. 9 shows the effect of imperfect CSI at the transmitter for various channel-to-error ratio (CER), which is defined as CER $\triangleq E[|h_{i,j}|^2]/\sigma_E^2$. For comparison, the performances with perfect CSI and without CSI are also plotted.[3] Clearly, as CER increases, the performance degradation due to imperfect CSI decreases and the performance converges to that with perfect CSI. As CER decreases, the performance converges to that without CSI. The reason is that when no CSI is available at the transmitter, any Tx filter that satisfies (3) achieves the same performance [5].

[3]The performance without CSI may be obtained with $\boldsymbol{T} = [I_K\ \ 0]^T$.

VII. Conclusion

In this paper, we have investigated the design of transmit (Tx) and receive (Rx) filters for the MIMO system in the sense of minimizing the BEP. We have derived the optimum Tx and Rx filters when the number of data symbols is two. For a general number of data symbols, we have derived a Tx and Rx filters design criterion referred to as equal SNIR criterion, and proposed Tx and Rx filters based on this equal SNIR criterion. The BEP performance of the proposed filter has been compared with that of the MMSE filter, and it was found that the proposed filter provides a significant improvement in BEP over the MMSE filter. This performance improvement is observed to decrease as the number of Tx antennas N_T increases for a fixed number of Rx antennas N_R, or as N_R increases for a fixed N_T. On the other hand, when both N_T and N_R increase, the BEP performance improvement increases significantly. Along with the BEP performance improvement, the proposed filter provides spectral efficiency improvement over the MMSE filter. It was found that even though the proposed filter was designed to minimize the BEP, the spectral efficiency of the proposed filter converges to the optimum water-filling capacity when the TxSNR increases.

Appendix A

In this appendix, (12) is derived. From (9), $\boldsymbol{\Phi}_k$ may be expressed as

$$\begin{aligned}\boldsymbol{\Phi}_k &= \frac{1}{\Gamma}\boldsymbol{I}_N + \sum_{i=k+1}^{K} (\boldsymbol{H}\boldsymbol{t}_i)(\boldsymbol{H}\boldsymbol{t}_i)^H \\ &= \frac{1}{\Gamma}\boldsymbol{I}_N + \sum_{i=k+2}^{K} (\boldsymbol{H}\boldsymbol{t}_i)(\boldsymbol{H}\boldsymbol{t}_i)^H + (\boldsymbol{H}\boldsymbol{t}_{k+1})(\boldsymbol{H}\boldsymbol{t}_{k+1})^H \\ &= \boldsymbol{\Phi}_{k+1} + (\boldsymbol{H}\boldsymbol{t}_{k+1})(\boldsymbol{H}\boldsymbol{t}_{k+1})^H. \end{aligned} \tag{A1}$$

The matrix inversion lemma states that

$$(\boldsymbol{A}+\boldsymbol{BDC})^{-1}=\boldsymbol{A}^{-1}-\boldsymbol{A}^{-1}\boldsymbol{B}(\boldsymbol{D}^{-1}+\boldsymbol{CA}^{-1}\boldsymbol{B})^{-1}\boldsymbol{CA}^{-1}. \tag{A2}$$

Thus, if we set $\boldsymbol{A}=\boldsymbol{\Phi}_{k+1}, \boldsymbol{B}=\boldsymbol{Ht}_{k+1}, \boldsymbol{C}=(\boldsymbol{Ht}_{k+1})^H$, and $\boldsymbol{D}=1$, then the inverse of $\boldsymbol{\Phi}_k$ can be expressed as

$$\boldsymbol{\Phi}_k^{-1}=\boldsymbol{\Phi}_{k+1}^{-1}-\frac{\boldsymbol{\Phi}_{k+1}^{-1}\boldsymbol{Ht}_{k+1}\boldsymbol{t}_{k+1}^H\boldsymbol{H}^H\boldsymbol{\Phi}_{k+1}^{-1}}{1+\left(\boldsymbol{t}_{k+1}^H\boldsymbol{H}^H\boldsymbol{\Phi}_{k+1}^{-1}\boldsymbol{Ht}_{k+1}\right)}. \tag{A3}$$

By recursion of (A3), $\boldsymbol{\Phi}_k^{-1}$ may be simplified as

$$\boldsymbol{\Phi}_k^{-1}=\boldsymbol{\Phi}_K^{-1}-\sum_{i=k+1}^{K}\frac{\boldsymbol{\Phi}_i^{-1}\boldsymbol{Ht}_i\boldsymbol{t}_i^H\boldsymbol{H}^H\boldsymbol{\Phi}_i^{-1}}{1+\left(\boldsymbol{t}_i^H\mathrm{H}^H\boldsymbol{\Phi}_i^{-1}\boldsymbol{Ht}_i\right)}. \tag{A5}$$

Finally, since $\boldsymbol{\Phi}_K^{-1}=\Gamma\boldsymbol{I}_{N_R}$, $\boldsymbol{\Phi}_k^{-1}$ may be expressed as

$$\boldsymbol{\Phi}_k^{-1}=\Gamma\boldsymbol{I}_{N_R}-\sum_{i=k+1}^{K}\frac{\boldsymbol{\Phi}_i^{-1}\boldsymbol{Ht}_i\boldsymbol{t}_i^H\boldsymbol{H}^H\boldsymbol{\Phi}_i^{-1}}{1+\left(\boldsymbol{t}_i^H\boldsymbol{H}^H\boldsymbol{\Phi}_i^{-1}\boldsymbol{Ht}_i\right)}. \tag{A6}$$

APPENDIX B

In this appendix, we show that the optimum $\boldsymbol{t}_2$ that minimizes (20) lies on the range space of $\boldsymbol{H}^H\boldsymbol{H}$ and may be expressed as $\boldsymbol{t}_2=\sqrt{q}\boldsymbol{v}_1+\sqrt{1-q}\boldsymbol{v}_2$, where q is a real number within the interval $[0,1]$. Since $\boldsymbol{t}_2$ is an $N_T\times 1$ vector, $\boldsymbol{t}_2$ may be expressed as the linear combination of N_T orthogonal bases, $\boldsymbol{v}_1, \boldsymbol{v}_2, \tilde{\boldsymbol{v}}_1, \tilde{\boldsymbol{v}}_2, \ldots$, and $\tilde{\boldsymbol{v}}_{N_T-2}$

$$\boldsymbol{t}_2=c_1\boldsymbol{v}_1+c_2\boldsymbol{v}_2+\sum_{i=1}^{N_T-2}\tilde{c}_i\tilde{\boldsymbol{v}}_i \tag{B1}$$

where $c_1, c_2, \tilde{c}_1, \tilde{c}_2, \ldots$, and $\tilde{c}_{N_T-2}$ are complex coefficients having the following constraint:

$$|c_1|^2+|c_2|^2+\sum_{i=1}^{N_T-2}|\tilde{c}_i|^2=1 \tag{B2}$$

to satisfy $\|\boldsymbol{t}_2\|^2=1$. Substituting $\boldsymbol{t}_2$ into (19), the matrix $\boldsymbol{A}(\boldsymbol{t}_2)$ can be expressed as

$$\begin{aligned}\boldsymbol{A}(\boldsymbol{t}_2)&=\boldsymbol{H}^H\boldsymbol{H}-\frac{\Gamma}{1+\Gamma\cdot\left(\boldsymbol{t}_2^H\boldsymbol{H}^H\boldsymbol{Ht}_2\right)}\left(\boldsymbol{H}^H\boldsymbol{Ht}_2\boldsymbol{t}_2^H\boldsymbol{H}^H\boldsymbol{H}\right)\\&=\boldsymbol{VBV}^H\end{aligned} \tag{B3}$$

where $\boldsymbol{B}$ is given as

$$\boldsymbol{B}=\begin{bmatrix}\lambda_1 & 0\\ 0 & \lambda_2\end{bmatrix}-\frac{\Gamma}{1+\Gamma\cdot(\lambda_1|c_1|^2+\lambda_2|c_2|^2)}\begin{bmatrix}\lambda_1^2|c_1|^2 & \lambda_1\lambda_2c_1c_2^*\\ \lambda_1\lambda_2c_1^*c_2 & \lambda_2^2|c_2|^2\end{bmatrix}.$$

The maximum eigenvalue of the 2×2 matrix $\begin{bmatrix}a & c\\ c^* & b\end{bmatrix}$ is given as

$$(1/2)(a+b+\sqrt{(a+b)^2-4(ab-|c|^2)}).$$

Thus, $\lambda_{\max}[\boldsymbol{B}]$ may be expressed as in (B4) at the bottom of the page, where ψ is given as $\psi=\Gamma/(1+\Gamma\cdot(\lambda_1|c_1|^2+\lambda_2|c_2|^2))$. Since $\boldsymbol{V}$ is an unitary matrix, we can easily show that $\lambda_{\max}[\boldsymbol{A}(\boldsymbol{t}_2)]$ is the same as $\lambda_{\max}[\boldsymbol{B}]$. Thus, the $\mathrm{SNIR}_1(\boldsymbol{t}_2)$ can be expressed as in (B5) at the bottom of the page.With $\boldsymbol{t}_2$ in (B1), the $\mathrm{SNIR}_2(\boldsymbol{t}_2)$ can be expressed as

$$\begin{aligned}\mathrm{SNIR}_2(\boldsymbol{t}_2)&=\Gamma\cdot\left(\boldsymbol{t}_2^H\boldsymbol{H}^H\boldsymbol{Ht}_2\right)\\&=\Gamma\cdot(\lambda_1|c_1|^2+\lambda_2|c_2|^2).\end{aligned} \tag{B6}$$

Note that only the amplitudes of c_1 and c_2 affect the $\mathrm{SNIR}_1(\boldsymbol{t}_2)$ and $\mathrm{SNIR}_1(\boldsymbol{t}_2)$. Thus, without loss of generality, we may set the phases of c_1 and c_2 to be zero. Hence, if we define Q as $Q\triangleq|c_1|^2+|c_2|^2$, then c_1 and c_2 may be expressed as

$$c_1=\sqrt{q} \tag{B7}$$

$$c_2=\sqrt{Q-q} \tag{B8}$$

where Q and q are real values with the constraints $0\le Q\le 1$ and $0\le q\le Q$. With these c_1 and c_2, the $\mathrm{SNIR}_1(\boldsymbol{t}_2)$ and $\mathrm{SNIR}_2(\boldsymbol{t}_2)$ may be expressed as in (B9) and (B10) at the top of the following page, where ψ is given as

$$\psi=\Gamma/\{1+\Gamma\cdot(\lambda_1q+\lambda_2(Q-q))\}.$$

Consider the partial derivatives of these $\mathrm{SNIR}_1(\boldsymbol{t}_2)$ and $\mathrm{SNIR}_2(\boldsymbol{t}_2)$ with respect to Q (see (B11) and (B12) also at the top of the following page). From the relations $\Gamma>0, \lambda_1\ge\lambda_2>0$, and $Q\ge q\ge 0$, it can be easily shown that $\partial\mathrm{SNIR}_1(\boldsymbol{t}_2)/\partial Q$ and $\partial\mathrm{SNIR}_2(\boldsymbol{t}_2)/\partial Q$ are larger than or equal to zero for any $\Gamma, \lambda_1, \lambda_2$, and q. Thus, the $\mathrm{SNIR}_1(\boldsymbol{t}_2)$ and $\mathrm{SNIR}_2(\boldsymbol{t}_2)$ are nondecreasing functions of Q, and their maximum values are achieved when $Q=1$. Thus, the optimum $\boldsymbol{t}_2$ may be obtained

$$\lambda_{\max}[\boldsymbol{B}]=\frac{1}{2}\left\{\lambda_1+\lambda_2-\psi\cdot\left(\lambda_1^2|c_1|^2+\lambda_2^2|c_2|^2\right)+\sqrt{\left(\lambda_1+\lambda_2-\psi\cdot(\lambda_1^2|c_1|^2+\lambda_2^2|c_2|^2)\right)^2-4\lambda_1\lambda_2\left(1-\psi\cdot(\lambda_1|c_1|^2+\lambda_2|c_2|^2)\right)}\right\} \tag{B4}$$

$$\begin{aligned}\mathrm{SNIR}_1(\boldsymbol{t}_2)&=\Gamma\cdot\lambda_{\max}[A(t_2)]=\Gamma\cdot\lambda_{\max}[\boldsymbol{B}]\\&=\frac{\Gamma}{2}\left\{\lambda_1+\lambda_2-\psi\cdot\left(\lambda_1^2|c_1|^2+\lambda_2^2|c_2|^2\right)+\sqrt{\left(\lambda_1+\lambda_2-\psi\cdot(\lambda_1^2|c_1|^2+\lambda_2^2|c_2|^2)\right)^2-4\lambda_1\lambda_2(1-\psi\cdot(\lambda_1|c_1|^2+\lambda_2|c_2|^2))}\right\}.\end{aligned} \tag{B5}$$

$$\mathrm{SNIR}_1(\boldsymbol{t}_2) = \frac{\Gamma}{2}\left\{\left(\lambda_1+\lambda_2-\psi\cdot\left(\lambda_1^2 q+\lambda_2^2(Q-q)\right)\right) + \sqrt{\left(\lambda_1+\lambda_2-\psi\cdot(\lambda_1^2 q+\lambda_2^2(Q-q))\right)^2 - 4\lambda_1\lambda_2(1-\psi\cdot(\lambda_1 q+\lambda_2(Q-q)))}\right\} \quad \text{(B9)}$$

$$\mathrm{SNIR}_2(t_2) = \Gamma\cdot(\lambda_1 q+\lambda_2(Q-q)) \quad \text{(B10)}$$

$$\frac{\partial \mathrm{SNIR}_1(t_2)}{\partial Q} = \frac{\psi^2}{2\Gamma}\left\{\Gamma\lambda_1(\lambda_1-\lambda_2)q-\lambda_2+\frac{\lambda_2(\lambda_1-\lambda_2+\Gamma\lambda_1\lambda_2 Q)+\Gamma\lambda_1(\lambda_1-\lambda_2)(\lambda_1+3\lambda_2+\Gamma\lambda_1\lambda_2 Q)q}{\sqrt{(\lambda_1-\lambda_2+\Gamma\lambda_1\lambda_2 Q)^2-4\Gamma\lambda_1\lambda_2(\lambda_1-\lambda_2)q}}\right\} \quad \text{(B11)}$$

$$\frac{\partial \mathrm{SNIR}_2(t_2)}{\partial Q} = \Gamma\cdot\lambda_2. \quad \text{(B12)}$$

when $Q=1$. In this case, the coefficients $\tilde{c}_1, \tilde{c}_2, \ldots$ and $\tilde{c}_{N_T-2}$ must satisfy

$$\sum_{i=1}^{N_T-2}|\tilde{c}_i|^2 = 1-(|c_1|^2+|c_2|^2) = 1-Q = 0. \quad \text{(B13)}$$

Hence, for the optimum $\boldsymbol{t}_2$, the coefficients $\tilde{c}_1, \tilde{c}_2, \ldots$ and $\tilde{c}_{N_T-2}$ should be 0. Consequently, the optimum $\boldsymbol{t}_2$ lies on the range space of $\boldsymbol{H}^H\boldsymbol{H}$, and may be expressed as $\boldsymbol{t}_2 = \sqrt{q}\boldsymbol{v}_1+\sqrt{1-q}\boldsymbol{v}_2$.

APPENDIX C

In this appendix, (30) is derived. Suppose that the matrix $\boldsymbol{T}^H\boldsymbol{H}^H\boldsymbol{H}\boldsymbol{T}$ may be written as the product of $\boldsymbol{U}$ and $\boldsymbol{L}$: $\boldsymbol{T}^H\boldsymbol{H}^H\boldsymbol{H}\boldsymbol{T} = \boldsymbol{U}\cdot\boldsymbol{L}$ where $\boldsymbol{U}=[\alpha_{i,j}]$ is an upper triangular matrix ($\alpha_{i,j}=0$ for $i>j$) and $\boldsymbol{L}=[\beta_{i,j}]$ is a lower triangular matrix ($\beta_{i,j}=0$ for $i<j$). Without loss of generality, we may set $\beta_{i,i}=1/\Gamma$ for $i=1,2,\ldots,K$. Then we can obtain $\alpha_{i,j}$ and $\beta_{i,j}$ through back substitution as

$$\alpha_{i,j} = \Gamma\left(\boldsymbol{t}_i^H\boldsymbol{H}^H\boldsymbol{H}\boldsymbol{t}_j - \sum_{n=j+1}^{K}\alpha_{i,n}\beta_{n,j}\right), \qquad i\le j \quad \text{(C1)}$$

$$\beta_{i,j} = \frac{1}{\alpha_{i,i}}\left(\boldsymbol{t}_i^H\boldsymbol{H}^H\boldsymbol{H}\boldsymbol{t}_j - \sum_{n=i+1}^{K}\alpha_{i,n}\beta_{n,j}\right), \qquad i\ge j. \quad \text{(C2)}$$

Note that in $\alpha_{i,n}$, there is the term $\boldsymbol{t}_i^H\boldsymbol{H}^H$ on its left side, and in $\beta_{n,j}$, the term $\boldsymbol{H}\boldsymbol{T}_j$ on its right side. Hence, we may simplify $\alpha_{i,j}$ and $\beta_{i,j}$ as $\alpha_{i,j} = \boldsymbol{t}_i^H\boldsymbol{H}^H\boldsymbol{F}_j\boldsymbol{H}\boldsymbol{t}_j$ and $\beta_{i,j} = (1)/(\alpha_{i,i})\boldsymbol{t}_i^H\boldsymbol{H}^H\boldsymbol{F}_i\boldsymbol{H}\boldsymbol{t}_j$ where $\boldsymbol{F}_j$ may be obtained by solving the equation

$$\begin{aligned}\alpha_{i,j} &= \boldsymbol{t}_i^H\boldsymbol{H}^H\boldsymbol{F}_j\boldsymbol{H}\boldsymbol{t}_j \\ &= \Gamma\left(\boldsymbol{t}_i^H\boldsymbol{H}^H\boldsymbol{H}\boldsymbol{t}_j - \sum_{n=j+1}^{K}\alpha_{i,n}\beta_{n,j}\right) \\ &= \Gamma\left(\boldsymbol{t}_i^H\boldsymbol{H}^H\boldsymbol{H}\boldsymbol{t}_j - \sum_{n=j+1}^{K}\boldsymbol{t}_i^H\boldsymbol{H}^H\boldsymbol{F}_n\boldsymbol{H}\boldsymbol{t}_n \cdot \frac{1}{\alpha_{n,n}}\boldsymbol{t}_n^H\boldsymbol{H}^H\boldsymbol{F}_n\boldsymbol{H}\boldsymbol{t}_j\right) \\ &= \boldsymbol{t}_i^H\boldsymbol{H}^H\left(\Gamma\boldsymbol{I}_{N_R} - \sum_{n=j+1}^{K}\frac{\boldsymbol{F}_n\boldsymbol{H}\boldsymbol{t}_n\boldsymbol{t}_n^H\boldsymbol{H}^H\boldsymbol{F}_n}{\boldsymbol{t}_n^H\boldsymbol{H}^H\boldsymbol{F}_n\boldsymbol{H}\boldsymbol{t}_n}\right)\boldsymbol{H}\boldsymbol{t}_j\end{aligned} \quad \text{(C3)}$$

and may be expressed

$$\boldsymbol{F}_j = \Gamma\boldsymbol{I}_{N_R} - \sum_{n=j+1}^{K}\frac{\boldsymbol{F}_n\boldsymbol{H}\boldsymbol{t}_n\boldsymbol{t}_n^H\boldsymbol{H}^H\boldsymbol{F}_n}{\boldsymbol{t}_n^H\boldsymbol{H}^H\boldsymbol{F}_n\boldsymbol{H}\boldsymbol{t}_n}. \quad \text{(C4)}$$

Note that $\boldsymbol{F}_j$ has the same form with the approximated $\boldsymbol{\Phi}_j^{-1}$ given in (28). Hence, we may further simplify $\alpha_{i,j}$ and $\beta_{i,j}$ as $\alpha_{i,j} = \boldsymbol{t}_i^H\boldsymbol{H}^H\boldsymbol{\Phi}_j^{-1}\boldsymbol{H}\boldsymbol{t}_j$ and $\beta_{i,j} = (1)/(\alpha_{i,i})\boldsymbol{t}_i^H\boldsymbol{H}^H\boldsymbol{\Phi}_i^{-1}\boldsymbol{H}\boldsymbol{t}_j$. Moreover, $\alpha_{k,k}$ becomes the same with the approximated SNIR_k given in (29)

$$\begin{aligned}\alpha_{k,k} &= \boldsymbol{t}_k^H\boldsymbol{H}^H\boldsymbol{\Phi}_k^{-1}\boldsymbol{H}\boldsymbol{t}_k \\ &= \boldsymbol{t}_k^H\boldsymbol{H}^H\left[\Gamma\boldsymbol{I}_{N_R} - \sum_{i=k+1}^{K}\frac{\boldsymbol{\Phi}_i^{-1}\boldsymbol{H}\boldsymbol{t}_i\boldsymbol{t}_i^H\boldsymbol{H}^H\boldsymbol{\Phi}_i^{-1}}{\boldsymbol{t}_i^H\boldsymbol{H}^H\boldsymbol{\Phi}_i^{-1}\boldsymbol{H}\boldsymbol{t}_i}\right]\boldsymbol{H}\boldsymbol{t}_k \\ &= \Gamma\left(\boldsymbol{t}_k^H\boldsymbol{H}^H\boldsymbol{H}\boldsymbol{t}_k\right) - \sum_{i=k+1}^{K}\frac{\left|\boldsymbol{t}_k^H\boldsymbol{H}^H\boldsymbol{\Phi}_i^{-1}\boldsymbol{H}\boldsymbol{t}_i\right|^2}{\boldsymbol{t}_i^H\boldsymbol{H}^H\boldsymbol{\Phi}_i^{-1}\boldsymbol{H}\boldsymbol{t}_i} \\ &= \mathrm{SNIR}_k.\end{aligned} \quad \text{(C5)}$$

With the above decomposition of $\boldsymbol{T}^H\boldsymbol{H}^H\boldsymbol{H}\boldsymbol{T}$, $\det[\boldsymbol{T}^H\boldsymbol{H}^H\boldsymbol{H}\boldsymbol{T}]$ may be expressed as

$$\begin{aligned}\det\left[\boldsymbol{T}^H\boldsymbol{H}^H\boldsymbol{H}\boldsymbol{T}\right] &= \det[\boldsymbol{U}\cdot\boldsymbol{L}] = \det[\boldsymbol{U}]\cdot\det[\boldsymbol{L}] \\ &= \left(\prod_{k=1}^{K}\alpha_{k,k}\right)\cdot\left(\prod_{k=1}^{K}\beta_{k,k}\right) \\ &= \frac{1}{\Gamma^K}\left(\prod_{k=1}^{K}\mathrm{SNIR}_k\right).\end{aligned} \quad \text{(C6)}$$

Hence, for high TxSNR, it holds that

$$\prod_{k=1}^{K}\mathrm{SNIR}_k = \Gamma^K\cdot\det[\boldsymbol{T}^H\boldsymbol{H}^H\boldsymbol{H}\boldsymbol{T}].$$

APPENDIX D

In this appendix, we show that if

$$\prod_{k=1}^{K}\mathrm{SNIR}_k \le \Gamma^K\cdot\prod_{k=1}^{K}\lambda_k$$

then the BEP cost function $J(\boldsymbol{t}_1, \boldsymbol{t}_2, \ldots, \boldsymbol{t}_K)$ in (13) is minimized when

$$\prod_{k=1}^{K} \mathrm{SNIR}_k = \Gamma^K \cdot \prod_{k=1}^{K} \lambda_k$$

and

$$\mathrm{SNIR}_1 = \mathrm{SNIR}_2 = \cdots = \mathrm{SNIR}_K.$$

Let $\mathrm{SNIR}_k = x_k$ and $\Gamma^K \cdot \prod_{k=1}^{K} \lambda_k = c$. Then the minimization of the BEP cost function $J(\boldsymbol{t}_1, \boldsymbol{t}_2, \ldots, \boldsymbol{t}_K)$ in (13) may be expressed as

$$\arg \min_{x_1, x_2, \ldots, x_K} \left\{ \sum_{k=1}^{K} Q(\sqrt{b \cdot x_k}) \right\} \quad \text{subject to} \quad \prod_{k=1}^{K} x_k \le c. \tag{D1}$$

where b is given as $3/(M-1)$. Using the Lagrange multiplier techniques, the Lagrangian may be expressed as

$$L(\mu, x_1, x_2, \ldots, x_K) = \left\{ \sum_{k=1}^{K} Q(\sqrt{b \cdot x_k}) \right\} + \mu \left\{ \prod_{k=1}^{K} x_k - c \right\} \tag{D2}$$

and its partial derivatives may be expressed as

$$\frac{\partial L(\mu, x_1, x_2, \ldots, x_K)}{\partial x_k} = -\frac{b}{\sqrt{8\pi b}} \frac{\exp(-b x_k/2)}{\sqrt{x_k}} + \mu \prod_{\substack{i=1 \\ i \ne k}}^{K} x_i. \tag{D3}$$

Setting all the partial derivatives to 0, we have

$$\mu = \frac{b}{\sqrt{8\pi b}} \frac{\sqrt{x_1} \exp(-b x_1/2)}{c} = \frac{b}{\sqrt{8\pi b}} \frac{\sqrt{x_2} \exp(-b x_2/2)}{c} = \cdots = \frac{b}{\sqrt{8\pi b}} \frac{\sqrt{x_K} \exp(-b x_K/2)}{c}. \tag{D4}$$

This implies that the condition $x_1 = x_2 = \cdots = x_K$ is a sufficient condition to minimize $J(\boldsymbol{t}_1, \boldsymbol{t}_2, \ldots, \boldsymbol{t}_K)$. Moreover, since $J(\boldsymbol{t}_1, \boldsymbol{t}_2, \ldots, \boldsymbol{t}_K)$ is a decreasing function of SNIR_k, $J(\boldsymbol{t}_1, \boldsymbol{t}_2, \ldots, \boldsymbol{t}_K)$ is minimized when $\prod_{k=1}^{K} \mathrm{SNIR}_k = c$. Consequently, the BEP cost function $J(\boldsymbol{t}_1, \boldsymbol{t}_2, \ldots, \boldsymbol{t}_K)$ in (13) is minimized when

$$\prod_{k=1}^{K} \mathrm{SNIR}_k = \Gamma^K \cdot \prod_{k=1}^{K} \lambda_k$$

and

$$\mathrm{SNIR}_1 = \mathrm{SNIR}_2 = \cdots = \mathrm{SNIR}_K.$$

Appendix E

In this appendix, (32) and (33) are derived. We first show that the term $\boldsymbol{t}_k^H \boldsymbol{H}^H \boldsymbol{\Phi}_i^{-1} \boldsymbol{H} \boldsymbol{t}_i$ in (11) may be expressed as $\boldsymbol{t}_k^H \boldsymbol{H}^H \boldsymbol{\Phi}_i^{-1} \boldsymbol{H} \boldsymbol{t}_i = \Gamma \cdot \boldsymbol{t}_k^H \boldsymbol{H}^H \boldsymbol{H} \boldsymbol{t}_i$ using the following mathematical induction.

i) For $i = K$, it is true that $\boldsymbol{t}_k^H \boldsymbol{H}^H \boldsymbol{\Phi}_i^{-1} \boldsymbol{H} \boldsymbol{t}_i = \Gamma \cdot \boldsymbol{t}_k^H \boldsymbol{H}^H \boldsymbol{H} \boldsymbol{t}_i$ since $\boldsymbol{\Phi}_K^{-1} = \Gamma \cdot \boldsymbol{I}_{N_R}$.

ii) Assume that $\boldsymbol{t}_k^H \boldsymbol{H}^H \boldsymbol{\Phi}_i^{-1} \boldsymbol{H} \boldsymbol{t}_i = \Gamma \cdot \boldsymbol{t}_k^H \boldsymbol{H}^H \boldsymbol{H} \boldsymbol{t}_i$ is true for $i = K, K-1, \ldots n+1$. Consider the term $\boldsymbol{t}_k^H \boldsymbol{H}^H \boldsymbol{\Phi}_i^{-1} \boldsymbol{H} \boldsymbol{t}_i$ when $i = n$. From the relation of (12), $\boldsymbol{t}_k^H \boldsymbol{H}^H \boldsymbol{\Phi}_n^{-1} \boldsymbol{H} \boldsymbol{t}_n$ can be expressed as

$$\boldsymbol{t}_k^H \boldsymbol{H}^H \boldsymbol{\Phi}_n^{-1} \boldsymbol{H} \boldsymbol{t}_n = \Gamma \cdot \boldsymbol{t}_k^H \boldsymbol{H}^H \boldsymbol{H} \boldsymbol{t}_n - \sum_{j=n+1}^{K} \frac{\left(\boldsymbol{t}_k^H \boldsymbol{H}^H \boldsymbol{\Phi}_j^{-1} \boldsymbol{H} \boldsymbol{t}_j\right) \cdot \left(\boldsymbol{t}_j^H \boldsymbol{H}^H \boldsymbol{\Phi}_j^{-1} \boldsymbol{H} \boldsymbol{t}_n\right)}{1 + \boldsymbol{t}_k^H \boldsymbol{H}^H \boldsymbol{\Phi}_j^{-1} \boldsymbol{H} \boldsymbol{t}_j}. \tag{E1}$$

Note that, from the assumption, the term $\boldsymbol{t}_k^H \boldsymbol{H}^H \boldsymbol{\Phi}_j^{-1} \boldsymbol{H} \boldsymbol{t}_j$ in (E1) may be expressed as

$$\boldsymbol{t}_k^H \boldsymbol{H}^H \boldsymbol{\Phi}_j^{-1} \boldsymbol{H} \boldsymbol{t}_j = \Gamma \cdot \boldsymbol{t}_k^H \boldsymbol{H}^H \boldsymbol{H} \boldsymbol{t}_j.$$

Similarly, the term $\boldsymbol{t}_j^H \boldsymbol{H}^H \boldsymbol{\Phi}_j^{-1} \boldsymbol{H} \boldsymbol{t}_{n-1}$ in (E1) can be expressed as

$$\boldsymbol{t}_j^H \boldsymbol{H}^H \boldsymbol{\Phi}_j^{-1} \boldsymbol{H} \boldsymbol{t}_{n-1} = \Gamma \cdot \boldsymbol{t}_j^H \boldsymbol{H}^H \boldsymbol{H} \boldsymbol{t}_{n-1}.$$

Hence, $\boldsymbol{t}_k^H \boldsymbol{H}^H \boldsymbol{\Phi}_n^{-1} \boldsymbol{H} \boldsymbol{t}_n$ may be simplified as

$$\boldsymbol{t}_k^H \boldsymbol{H}^H \boldsymbol{\Phi}_n^{-1} \boldsymbol{H} \boldsymbol{t}_n = \Gamma \cdot \boldsymbol{t}_k^H \boldsymbol{H}^H \boldsymbol{H} \boldsymbol{t}_n - \sum_{j=n+1}^{K} \frac{\Gamma^2 \cdot \boldsymbol{t}_k^H \boldsymbol{H}^H \boldsymbol{H} \boldsymbol{t}_j \cdot \boldsymbol{t}_j^H \boldsymbol{H}^H \boldsymbol{H} \boldsymbol{t}_n}{1 + \boldsymbol{t}_k^H \boldsymbol{H}^H \boldsymbol{\Phi}_j^{-1} \boldsymbol{H} \boldsymbol{t}_j}. \tag{E2}$$

Note that, for $\boldsymbol{t}_a$ and $\boldsymbol{t}_b$ that lie in different 2-D range subspaces of $\boldsymbol{H}^H \boldsymbol{H}$, it is true that $\boldsymbol{t}_a^H \boldsymbol{H}^H \boldsymbol{H} \boldsymbol{t}_b = 0$. Note also that three Tx weight vectors, $\boldsymbol{t}_k, \boldsymbol{t}_j$ and $\boldsymbol{t}_n$, cannot lie simultaneously within the same 2-D range subspace, since we assume that only two Tx weight vectors lie in one 2-D range subspace. Hence, at least one of $\boldsymbol{t}_k^H \boldsymbol{H}^H \boldsymbol{H} \boldsymbol{t}_j$ and $\boldsymbol{t}_j^H \boldsymbol{H}^H \boldsymbol{H} \boldsymbol{t}_{n-1}$ in (E2) becomes zero. Consequently, $\boldsymbol{t}_k^H \boldsymbol{H}^H \boldsymbol{\Phi}_n^{-1} \boldsymbol{H} \boldsymbol{t}_n$ may be simplified as

$$\boldsymbol{t}_k^H \boldsymbol{H}^H \boldsymbol{\Phi}_n^{-1} \boldsymbol{H} \boldsymbol{t}_n = \Gamma \cdot \boldsymbol{t}_k^H \boldsymbol{H}^H \boldsymbol{H} \boldsymbol{t}_n. \tag{E3}$$

Thus, it is true that $\boldsymbol{t}_k^H \boldsymbol{H}^H \boldsymbol{\Phi}_i^{-1} \boldsymbol{H} \boldsymbol{t}_i = \Gamma \cdot t_k^H \boldsymbol{H}^H \boldsymbol{H} \boldsymbol{t}_i$ for $i = n$.

From i) and ii), the term $\boldsymbol{t}_k^H \boldsymbol{H}^H \boldsymbol{\Phi}_i^{-1} \boldsymbol{H} \boldsymbol{t}_i$ may be expressed as $\boldsymbol{t}_k^H \boldsymbol{H}^H \boldsymbol{\Phi}_i^{-1} \boldsymbol{H} \boldsymbol{t}_i = \Gamma \cdot \boldsymbol{t}_k^H \boldsymbol{H}^H \boldsymbol{H} \boldsymbol{t}_i$. Moreover, when $\boldsymbol{t}_k$ and $\boldsymbol{t}_i$ lie in different 2-D range subspaces of $\boldsymbol{H}^H \boldsymbol{H}$, then $\boldsymbol{t}_k^H \boldsymbol{H}^H \boldsymbol{H} \boldsymbol{t}_i$ becomes zero. Hence, from the above observations and (11), SNIR_{1+m} and SNIR_{K-m} may be expressed as

$$\mathrm{SNIR}_{1+m} = \Gamma \cdot \left(\boldsymbol{t}_{1+m}^H \boldsymbol{H}^H \boldsymbol{H} \boldsymbol{t}_{1+m}\right) - \frac{\Gamma^2 \cdot \left|\boldsymbol{t}_{1+m}^H \boldsymbol{H}^H \boldsymbol{H} \boldsymbol{t}_{K-m}\right|^2}{1 + \Gamma \cdot \left(\boldsymbol{t}_{K-m}^H \boldsymbol{H}^H \boldsymbol{H} \boldsymbol{t}_{K-m}\right)} \tag{E4}$$

$$\mathrm{SNIR}_{K-m} = \Gamma \cdot \left(\boldsymbol{t}_{K-m}^H \boldsymbol{H}^H \boldsymbol{H} \boldsymbol{t}_{K-m}\right). \tag{E5}$$

Appendix F

In this appendix, we show that when the optimum Tx and Rx filters for $K = 2$ given in (24)–(27) are applied, the corresponding SNIRs may be expressed for high TxSNR as $\mathrm{SNIR}_1 \cong \mathrm{SNIR}_2 \cong \Gamma\sqrt{\lambda_1 \lambda_2}$. Note that the SNIRs with the proposed filter may be obtained from (21) and (22) by replacing q with q_{opt} : $\mathrm{SNIR}_1(q_{\mathrm{opt}})$ and $\mathrm{SNIR}_2(q_{\mathrm{opt}})$. For high TxSNR, $\psi(q)$ in (21) may be approximated as $\psi(q) \cong 1/(\lambda_1 q + \lambda_2(1-q))$, with which, the $\mathrm{SNIR}_1(q)$ in (21) may be approximated as

$$\mathrm{SNIR}_1(q) \cong \frac{\Gamma \lambda_1 \lambda_2}{\lambda_1 q + \lambda_2 (1-q)}. \tag{F1}$$

From (F1) and (22), the product of $\mathrm{SNIR}_1(q)$ and $\mathrm{SNIR}_2(q)$ is found as

$$\mathrm{SNIR}_1(q) \cdot \mathrm{SNIR}_2(q) \cong \Gamma^2 \lambda_1 \lambda_2. \tag{F2}$$

Observe that the product of $\mathrm{SNIR}_1(q)$ and $\mathrm{SNIR}_2(q)$ does not depend on q, and may be considered as a constant value. In this case, from Appendix D, the cost function $J(q)$ in (23) is minimized when $\mathrm{SNIR}_1(q) = \mathrm{SNIR}_2(q)$. Hence, for high TxSNR, the optimum q may be obtained by solving $\mathrm{SINR}_1(q) = \mathrm{SINR}_2(q)$ as follows:

$$q_{\mathrm{opt}} \cong \frac{\sqrt{\lambda_2}}{\sqrt{\lambda_1} + \sqrt{\lambda_2}}. \tag{F3}$$

Substituting (F3) into (F1) and (22), $\mathrm{SNIR}_1(q_{\mathrm{opt}})$ and $\mathrm{SNIR}_2(q_{\mathrm{opt}})$ may be obtained as

$$\mathrm{SNIR}_1(q_{\mathrm{opt}}) \cong \Gamma\sqrt{\lambda_1 \lambda_2} \tag{F4}$$

$$\mathrm{SNIR}_2(q_{\mathrm{opt}}) \cong \Gamma\sqrt{\lambda_1 \lambda_2}. \tag{F5}$$

This indicates that when the optimum Tx and Rx filters for $K = 2$ are applied, the corresponding SNIRs may be expressed for high TxSNR as $\mathrm{SNIR}_1 \cong \mathrm{SNIR}_2 \cong \Gamma\sqrt{\lambda_1 \lambda_2}$.

References

[1] E. Telatar, "Capacity of multi-antenna Gaussian channels," AT&T Bell Labs. Tech. Memo., Mar. 1995.

[2] G. J. Foschini and M. J. Gans, "On limits of wireless communications in a fading environment when using multiple antennas," *Wireless Personal Commun.*, vol. 6, no. 3, pp. 311–335, Mar. 1998.

[3] G. J. Foschini, G. D. Golden, R. A. Valenzuela, and P. W. Wolniansky, "Simplified processing for high spectral efficiency wireless communication employing multi-element arrays," *IEEE J. Sel. Areas Commun.*, vol. 17, no. 11, pp. 1841–1852, Nov. 1999.

[4] V. Tarokh, N. Seshadri, and A. R. Calderbank, "Space-time codes for high data rate wirelss communication: Performance criterion and code construction," *IEEE Trans. Inf. Theory*, vol. 44, no. 2, pp. 744–765, Mar. 1998.

[5] A. Narula, M. J. Lopez, M. D. Trott, and G. W. Wornell, "Efficient use of side information in multiple antenna data transmission over fading channels," *IEEE J. Sel. Areas Commun.*, vol. 16, no. 10, pp. 1423–1436, Oct. 1998.

[6] J. Salz, "Digital transmission over cross-coupled linear channels," *AT&T Tech. J.*, vol. 64, pp. 1147–1159, July 1985.

[7] J. Yang and S. Roy, "On joint transmitter and receiver optimization for multi-input-multi-output (MIMO) transmission systems," *IEEE Trans. Commun.*, vol. 42, no. 12, pp. 3221–3231, Dec. 1994.

[8] A. Scaglione, G. B. Giannakis, and S. Barbarossa, "Redundant filterbank precoder and equalizer part I: Unification and optiamal designs," *IEEE Trans. Signal Process.*, vol. 47, no. 7, pp. 1988–2006, July 1999.

[9] H. Sampath and A. Paulraj, "Joint transmit and receive optimization for high data rate wireless communications using multiple antennas," in *Proc. Asilomar Conf. Signals, Systems, and Computers*, vol. 1, Pacific Grove, CA, 1999, pp. 215–219.

[10] H. Sampath, P. Stoica, and A. Paulraj, "Generalized precoder and decoder design for MIMO channels using the weighted MMSE criterion," *IEEE Trans. Commun.*, vol. 49, no. 12, pp. 2198–2206, Dec. 2001.

[11] C.-C. Yeh and J. R. Barry, "Adaptive minimum bit-error rate equalization for binary signaling," *IEEE Trans. Commun.*, vol. 48, no. 7, pp. 1226–1235, July 2000.

[12] J. G. Proakis, *Digital Communication*, 3rd ed. New York: McGraw-Hill, 1995.

[13] M. K. Simon, S. M. Hinedi, and W. C. Lindsey, *Digital Communication Techniques*. Englewood Cliffs, NJ: Prentice-Hall, 1995.

[14] R. A. Monzingo and T. W. Miller, *Introduction to Adaptive Arrays*. New York, NY: Wiley, 1980.

[15] G. Strang, *Linear Algebra and Its Applications*, 3rd ed. Fort Worth, TX: Harcourt Brace, 1988.

[16] S. Boyd and L. Vandenberghe, *Convex Optimization*. Cambridge, U.K.: Cambridge Univ. Press, 2004.

[17] R. A. Horn and C. R. Johnson, *Matrix Analysis*. Cambridge, U.K.: Cambridge Univ. Press, 1985.

[18] W. H. Press *et al.*, *Numerical Recipes in C*, 2nd ed. Cambridge, U.K.: Cambridge Univ. Press, 1992.

[19] A. Edelman, "Eigenvalues and condition numbers of random matrices," in *SIAM J. Matrix Analysis Applic.*, vol. 9, Oct. 1988, pp. 543–560.

[20] K. K. Wong, R. D. Murch, and K. B. Letaief, "Performance enhancement of multiuser MIMO wireless communication systems," *IEEE Trans. Commun.*, vol. 50, no. 12, pp. 1960–1970, Dec. 2002.

[21] G. G. Raleigh and J. M. Cioffi, "Spatio-temporal coding for wireless communications," *IEEE Trans. Commun.*, vol. 46, no. 3, pp. 357–366, Mar. 1998.

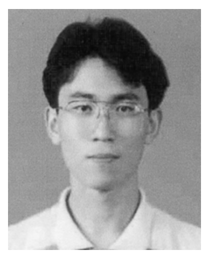

Keun Chul Hwang received the B.S., M.S., and Ph.D. degrees in electrical engineering from Seoul National University, Seoul, Korea, in 1997, 1999, and 2003, respectively.

From 2003 to 2004, he was with the Department of Electrical and Computer Engineering at The University of Texas at Austin, as a Postdoctoral Research Fellow. He is currently with Samsung Electronics Inc. His research interests include wireless communication and signal processing for multiple-antenna systems.

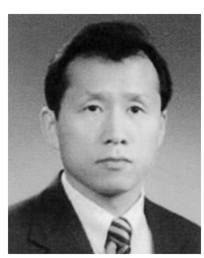

Kwang Bok (Ed) Lee (S'86–M'90) received the B.A.Sc. and M.Eng. degrees from the University of Toronto, Toronto, ON, Canada, in 1982 and 1986, respectively, and the Ph.D. degree from McMaster University, Hamilton, ON, Canada, in 1990.

He was with Motorola Canada from 1982 to 1985, and Motorola USA from 1990 to 1996 as a Senior Staff Engineer. At Motorola, he was involved in the research and development of wireless communication systems. He was with Bell-Northern Research, Ottawa, ON, Canada, from 1989 to 1990. In March 1996, he joined the School of Electrical Engineering, Seoul National University, Seoul, Korea. Currently, he is an Associate Professor in the School of Electrical Engineering. He was a Vice Chair of the School of Electrical Engineering from 2000 to 2002. He has been serving as a Consultant to a number of wireless industries. His research interests include mobile communications, communication technique covering physical layer and upper layer. He holds ten U.S. patents and four Korean patents, and has a number of patents pending.

Dr. Lee was an Editor of the IEEE JOURNAL ON SELECTED AREAS IN COMMUNICATIONS, Wireless Series in 2001, and has been an Editor of the IEEE TRANSACTIONS ON WIRELESS COMMUNICATIONS since 2002. He is a Co-Chair of the ICC2005 Wireless Communication Symposium. He received the Best Paper Award from CDMA International Conference 2000 (CIC 2000), and the Best Teacher Award in 2003 from College of Engineering, Seoul National University.